HHS Public Access

Author manuscript

Nat Immunol. Author manuscript; available in PMC 2023 September 05.

Published in final edited form as:

Nat Immunol. 2020 December ; 21(12): 1528–1539. doi:10.1038/s41590-020-0795-1.

Migration-induced cell shattering due to DOCK8-deficiency causes a type-2 biased helper T cell response

Caitlin Schneider[1,2], **Connie Shen**[1,2], **Angelica A. Gopal**[2,3,‡], **Todd Douglas**[1,2], **Benjamin Forestell**[1,2], **Keith D. Kauffman**[4], **Dakota Rogers**[2,3], **Patricio Artusa**[2,3], **Qian Zhang**[5,ϕ], **Huie Jing**[5], **Alexandra F. Freeman**[5], **Daniel L. Barber**[4], **Irah L. King**[6], **Maya Saleh**[7,§], **Paul W. Wiseman**[8], **Helen C. Su**[5], **Judith N. Mandl**[1,2,3,*]

[1]Department of Microbiology and Immunology, McGill University, Montreal, QC, Canada.

[2]McGill Research Centre for Complex Traits, McGill University, Montreal, QC, Canada.

[3]Department of Physiology, McGill University, Montreal, QC, Canada.

[4]T Lymphocyte Biology Unit, Laboratory of Parasitic Diseases, National Institute of Allergy and Infectious Diseases, National Institutes of Health, Bethesda, MD, USA.

[5]Laboratory of Clinical Immunology and Microbiology, National Institute of Allergy and Infectious Diseases, National Institutes of Health, Bethesda, MD, USA.

[6]Meakins-Christie Laboratories, Department of Microbiology and Immunology, McGill University Health Centre Research Institute, Montreal, QC, Canada.

[7]Department of Medicine, McGill University, Montreal, QC, Canada.

[8]Department of Chemistry and Department of Physics, McGill University, Montreal, QC, Canada.

Abstract

Mutations that impact immune cell migration and result in immune deficiency illustrate the importance of cell movement in host defense. In humans, loss-of-function mutations in *DOCK8*, a guanine exchange factor involved in hematopoietic cell migration, leads to immunodeficiency and, paradoxically, allergic disease. Here, we demonstrate that, like humans, *Dock8*$^{-/-}$ mice have a profound type-2 CD4^{+} T helper cell (Th2) bias upon pulmonary infection with *Cryptococcus neoformans* and other non-Th2 stimuli. We found that recruited *Dock8*$^{-/-}$ CX3CR1^{+} mononuclear

*To whom correspondence should be addressed: judith.mandl@mcgill.ca, Bellini Building, room 364, 3649 Promenade Sir William Osler, Montreal, QC, Canada H3G 0B1.

‡Current address: Massachusetts General Hospital, Boston, USA.

ϕCurrent address: St. Giles Laboratory of Human Genetics of Infectious Diseases, Rockefeller University, New York, USA

§Current address: University of Bordeaux, France.

Author Contributions

J.N.M. conceived the project. C.Sc. and J.N.M. designed the research. C.Sc. performed most experiments with critical help from C.Sh., B.F., K.D.K., P.A., and D.R. A.A.G. contributed some of the BMDC and T cell collagen matrix movies and associated analyses of cell shape with input from P.W.W. C.Sh. contributed the CFA experiments, with input from I.L.K., and higher resolution images and movies of migrating BMDC and T cells. T.D. performed the western blots for caspase activation with input from M.S. Data was analysed by J.N.M., C.Sc., A.A.G., C.Sh., M.S., and P.W.W. At NIH, A.F.F. and H.C.S. provided human samples that were processed and analyzed by H.J. Critical reagents and intellectual input was provided by I.L.K., M.S., D.L.B, Q.Z., and H.C.S. The manuscript was written by J.N.M. and C.Sc. with all authors contributing and providing feedback.

Competing Interests Statement

The authors declare no competing interests.

phagocytes are exquisitely sensitive to migration-induced cell shattering, releasing IL-1β that drives GM-CSF production by CD4$^+$ T cells. Blocking IL-1β, GM-CSF, or caspase activation eliminated the type-2 skew in mice lacking DOCK8. Importantly, treatment of infected wild-type mice with apoptotic cells significantly increased GM-CSF production and Th2 differentiation. This reveals an important role for cell death in driving type-2 signals during infection, which may have implications for understanding the etiology of type-2 CD4$^+$ T cell responses in allergic disease.

Introduction

Heritable defects in host defense can shed light on the molecular and cellular underpinnings of immune processes[1]. Highlighting the importance of cell movement to immune function, impaired immune cell migration underlies several identified primary immunodeficiencies, including those caused by mutations in *ITGB2, WASP, CORO1A, MST1, CXCR4*, and *DOCK8*[2, 3, 4, 5, 6]. Autosomal recessive loss-of-function mutations in *DOCK8* were originally identified in patients with low T cell counts in the blood, persistent viral and bacterial skin infections, mucosal fungal infections, and recurring respiratory infections[7, 8]. DOCK8 is an atypical guanine exchange factor that is expressed only in hematopoietic cells and activates Rho GTPases such as CDC42[9, 10, 11]. Loss of DOCK8 impairs the migration of T cells in dense 3D tissue environments which, given the density of the epidermis and dermis, may explain the particular susceptibility of DOCK8-deficient humans to skin infections[12]. Perhaps paradoxically, individuals with DOCK8-deficiency also have a high incidence of allergic diseases and eczema, hyper IgE, eosinophilia, and a higher proportion of CD4$^+$ T cells producing the type-2 cytokines IL-4 and IL-13[7, 13].

Other work has implicated DOCK8 in B cell immunological synapse formation[14]; CD8$^+$ T memory cell survival[15]; STAT3 translocation to the nucleus in group 3 innate lymphoid cells (ILC3s)[16]; STAT5 phosphorylation in T regulatory cells[17]; natural killer cell function[18]; actomyosin dynamics at the leading edge in migrating macrophages[19]; MyD88 signalling via TLR9 in B cells[20]; TCR-driven WASP activation[21]; LFA-1—ICAM adhesion of migrating T cells under shear conditions[21]; migration defects of CD11b$^+$ dendritic cell (DC) subsets and subsequent impaired induction of T follicular helper (Tfh) cell responses[22], and most recently in the generation of IL-13 producing Tfh cells which promote high affinity IgE production[23]. However, none of these identified functions explain why DOCK8 deficiency might result in CD4$^+$ T cells prone to allergic, type-2 responses.

Type-2 CD4$^+$ T helper (Th2) responses are characterized by their production of IL-4, IL-5 and IL-13, as well as expression of the lineage determining transcription factor GATA3[24, 25, 26]. They are critical for host protection against macroparasites such as helminths, but can lead to pathology and allergic hypersensitivities when arising in response to non-infectious antigens. It has been posited that one critical function of type-2 responses is a rapid reestablishment of tissue integrity through, for instance, the alternative activation of macrophages that stimulate tissue repair[27, 28]. In addition, Th2 cells promote tissue recruitment of eosinophils and the secretion of IgE which binds Fce receptors and activates mast cells and basophils, leading to vasodilation and smooth muscle peristalsis, as well

as increased mucus production, all of which contribute to eliciting expulsion mechanisms at barrier surfaces[24, 25, 26]. For this reason, it has also been proposed that, rather than being misdirected anti-parasitic responses, allergic reactions serve as signals that lead to an individual leaving an environment containing noxious substances, irritants or toxins, and thus type-2 allergic immune responses might share a common defense strategy with the purging of large pathogens[29].

Th2 responses are shaped both in secondary lymphoid organs (SLOs) during $CD4^+$ T cell priming, as well as through tissue-specific processes at the site of allergen or parasite introduction which can impact priming or subsequent amplification of the type-2 response[26, 30]. In SLOs, DCs expressing KLF4 are particularly important in eliciting Th2 responses, as is the cytokine milieu in which T cell priming takes place[26]. Moreover, weaker T cell receptor signals from interactions with peptide-MHC on antigen-presenting cells during T cell activation favor Th2 cell differentiation[30, 31]. In the lung, a major site of allergic responses, the release of the alarmins IL-25, thymic stromal lymphopoietin (TSLP), and IL-33 by epithelial cells, and of type-2 cytokines by group 2 innate lymphoid cells (ILC2s) can promote Th2 cell priming indirectly through their actions on DCs, or directly by polarizing recruited effector $CD4^+$ T cells[26, 32, 33]. Importantly, how divergent stimuli such as macroparasites, venoms, noxious compounds, and various allergens can elicit Th2 responses and what common signal might underlie the initiation of the same $CD4^+$ T cell effector response is still not well understood[25].

Here we investigated the mechanism for the Th2-biased $CD4^+$ T cell response *in vivo* in Dock8-deficient mice and identified cell death as a key signal leading to type-2 immunity. We show that lung-infiltrating *Dock8*$^{-/-}$ mononuclear phagocytes (MNPs) expressing the fractalkine receptor CX3CR1 are highly susceptible to migration-induced shattering (cytothripsis), releasing IL-1β in the process, and leading to GM-CSF production by $CD4^+$ T cells; we show that caspase-dependent cell death, along with IL-1β, are critical drivers for the type-2 bias.

Results

Dock8 deficiency leads to a type-2 differentiation bias in $CD4^+$ T cells

$CD4^+$ T cells isolated from DOCK8-deficient individuals have an increased frequency of cells producing IL-4 and IL-13 upon restimulation *ex vivo* (Fig. 1a), as previously observed[13]. To determine whether mice lacking Dock8 exhibit a Th2 bias similar to humans with loss-of-function mutations in *DOCK8*, we infected *Dock8*$^{-/-}$ mice with the opportunistic fungal pathogen *Cryptococcus neoformans*, which infects some *DOCK8*-deficient patients[7, 8]. $CD4^+$ T cells are critical for control of fungal dissemination to the CNS from the primary site of infection, the airway, with HIV-infected individuals being particularly susceptible to lethal *C. neoformans* infections[34, 35]. Pulmonary *Cryptococcus* infection elicits multiple T helper lineages, whereby a strong Th2 response is detrimental to, and a Th17 response is beneficial for, pathogen control [36, 37, 38].

Twenty days after pulmonary *C. neoformans* infection, we assessed $CD4^+$ T cell responses in the lung and found a significantly higher percentage of activated $CD4^+$ T cells producing

the Th2 cytokines IL-4, IL-5, and IL-13 in *Dock8*$^{-/-}$ mice (Fig. 1b, c). On average, in *Dock8*$^{-/-}$ mice CD4^{+} T cells making any combination of these Th2 cytokines were 2-3 fold more frequent (Fig. 1d). The strong Th2-biased response was apparent also when quantifying total numbers of Th2 cytokine-producing CD4^{+} T cell in the lung (Supplementary Fig. 1a,b). We observed a corresponding increase in expression of the Th2 lineage transcription factor GATA-3 in activated CD4^{+} T cells in the lung (Fig. 1e). Surprisingly, *Dock8*$^{-/-}$ mice had a significantly lower fungal burden in the lung (Fig. 1f), suggesting that they were better at controlling the pathogen during the first 20 days of infection despite the increased Th2 response. Upon longer-term infection, fungal dissemination to the spleen in wild type (WT) and *Dock8*$^{-/-}$ mice was similar, and there was a significantly higher fungal burden in the brains of *Dock8*$^{-/-}$ mice (Supplementary Fig. 1c). Yet, infected *Dock8*$^{-/-}$ mice lived significantly longer than WT mice (Supplementary Fig. 1d).

Although loss of Dock8 is associated with migration defects in a number of immune cell types[11, 12, 19, 22, 39], we observed significantly more cells infiltrating the lungs of *Dock8*$^{-/-}$ mice during *C. neoformans* infection (Fig. 1g). There were also significantly more eosinophils in *Dock8*$^{-/-}$ lungs, corroborating the robust Th2 response we observed (Fig. 1h). Hematoxylin and eosin (H&E) staining of lung tissue sections revealed large aggregates of inflammatory cells present around individual *Cryptococcus* cells in the lungs of *Dock8*$^{-/-}$ mice (Fig. 1i).

We and others have previously shown T cell intrinsic roles for DOCK8 in migration through tissue and vascular adhesion, impairing entry into lymphoid organs[12, 21]. Therefore, we examined whether differences in the activation and lung recruitment of CD4^{+} T cells might account for altered helper lineage differentiation. First, we compared CD4^{+} T cell numbers in non-draining (inguinal) lymph nodes (ndLN), dLN, and lung during *C. neoformans* infection. Consistent with the lymphopenia seen in DOCK8-deficient patients, CD4^{+} T cell counts were significantly lower in ndLNs (Supplementary Fig. 1e). There was no difference in total CD4^{+} T cell numbers or number of activated CD4^{+} T cells in the dLN, as would be expected given that *Dock8*$^{-/-}$ T cells have no defect in cell division[12], and we observed a significantly greater recruitment of CD4^{+} T cells to the lung in *Dock8*$^{-/-}$ mice (Supplementary Fig. 1f). To ascertain whether these lung CD4^{+} T cells were localized in the lung parenchyma or trapped in the blood vessels unable to extravasate[21], we injected a fluorophore-conjugated anti-CD45 antibody to fluorescently label all immune cells in the blood prior to harvesting the tissue for flow cytometry[40]. Nearly all CD4^{+} T cells were located in the lung parenchyma in Dock8$^{-/-}$ mice (Supplementary Fig. 1g).

Together, these observations show that *Dock8*$^{-/-}$ mice recapitulate the Th2 bias observed in DOCK8-deficient humans during *C. neoformans* infection and that this is not tied to a failure of CD4^{+} T cells to expand or to enter the site of infection.

Dock8-deficiency causes a type-2 biased CD4^{+} T cell response to non-Th2 stimuli

To more comprehensively interrogate the functionality of CD4^{+} T cells recruited to the lung following infection with *C. neoformans*, we evaluated production of 7 cytokines simultaneously by flow cytometry. We determined all possible cytokine combinations and

investigated which ones differed significantly between *Dock8*$^{-/-}$ and WT mice, a set of 25 combinations out of the possible 128. Interestingly, the most striking change in the functionality of CD4^{+} T cells in *Dock8*$^{-/-}$ mice was the increased frequency of cells producing GM-CSF, either alone or in combination with TNFα and any of the type-2 cytokines IL-4, IL-5, and IL-13 (Fig. 2a). Of note, the percentage of activated CD4^{+} T cells making IFNγ was not decreased, but rather increased slightly in Dock8-deficient cells relative to WT (Fig. 2b), suggesting that the Th2-bias was not the result of loss of counter-regulation by type-1 helper T cells. Indeed, levels of IL-12p70 were not different in total lung homogenate between WT and KO mice (Supplementary Fig. 2a), and nor was TNFα production by activated CD4^{+} T cells (Fig. 2b). As has been observed in DOCK8-deficient people[13], IL-17 production was significantly reduced in *Dock8*$^{-/-}$ mice (Fig. 2b). In accordance with our cytokine screen (Fig. 2a), there was a ~5-fold increase in the frequency of GM-CSF producing CD4^{+} T cells in the lungs of *Dock8*$^{-/-}$ mice compared to WT mice (Fig. 2b).

To determine whether *Dock8*$^{-/-}$ mice exhibit a Th2 skew upon infection even with a pathogen that strongly induces a Th1 response, we infected mice with influenza A virus. At the peak of the T cell response on day 7, we observed a lower number of activated CD4^{+} T cells in the lungs of KO mice (Supplementary Fig. 2b), compared to the greater numbers we observed 20 days post-infection with *C. neoformans* (Supplementary Fig. 1f). In contrast to the *C. neoformans* infections, during influenza virus infection we observed a significantly higher percentage of activated CD4^{+} T cells making IL-17 and a lower percentage making IFNγ in the KO compared to WT (Fig. 2c). However, as with *C. neoformans* there was no difference in the TNFα response and, importantly, there was a large increase in the percentage of activated CD4^{+} T cells producing Th2 cytokines in *Dock8*$^{-/-}$ mice as compared to the WT controls (Fig. 2c). Dock8$^{-/-}$ mice infected with influenza A had significantly increased eosinophil infiltration, as well as increased viral loads in the lung (Supplementary Fig. 2c,d), in line with the increased Th2 response.

To further confirm the generality of the Th2-bias of *Dock8*$^{-/-}$ mice, we immunized mice with Complete Freund's Adjuvant (CFA) and ovalbumin peptide and assessed the CD4^{+} T cell response in the iliac lymph node 7 days after injection. CFA immunization led to a similar expansion of activated CD4^{+} T cells in WT and *Dock8*$^{-/-}$ mice (Supplementary Fig. 2e). Moreover, as observed in *C. neoformans* and influenza virus infections, immunizing *Dock8*$^{-/-}$ mice led to a greater frequency of CD4^{+} T cells making IL-4, IL-5, and IL-13, as well as TNFα, while there was no difference in the frequency of cells producing IL-17 (Fig. 2d). Eosinophil recruitment to the lymph node was found to be the same between Dock8$^{-/-}$ and WT mice (Supplementary Fig. 2f).

To determine whether Dock8-deficiency, in addition to skewing a CD4^{+} T cell effector response to favour Th2 cytokine production, was also enhancing a Th2 response upon challenge with a pathogen that provides a strong type-2 stimulus, we orally infected mice with the helminth *Heligmosomoides polygyrus* and assessed the CD4^{+} T cell response in the gut-draining (mesenteric) lymph node 7 days later. *H. polygyrus* infection resulted in a similar expansion of activated CD4^{+} T cells between WT and KO mice (Supplementary Fig. 2g), and there was no difference between *Dock8*$^{-/-}$ and WT mice in the production of

IL-17, GM-CSF, TNFα, or the Th2 cytokines IL-4, IL-15, and IL-13 (Supplementary Fig. 2h). There was, however, a significant increase in IFNγ-producing activated CD4$^+$ T cells in KO mice (Supplementary Fig. 2h), and a significantly higher number of eosinophils in KO mesenteric lymph nodes (Supplementary Fig. 2i).

Overall our data suggest that Dock8-deficiency provides a type-2 inducing stimulus in infection and immunization settings that usually lead to non-Th2 effector CD4$^+$ T cell responses, but does not exacerbate the type-2 response in a Th2-inducing infection model.

Absence of Dock8 expression in CX3CR1$^+$ mononuclear phagocytes is sufficient to recapitulate the type-2 effector CD4$^+$ T cell bias

To begin to investigate the cell type(s) within which the Dock8-deficiency was driving the biased CD4$^+$ T cell response, we first confirmed whether the Th2 skew was a consequence of Dock8-deficiency in the hematopoietic compartment. Dock8 expression was previously shown to be restricted to hematopoietic cells, but this was only examined in the absence of infection[12]. We irradiated *Dock8*$^{-/-}$ mice, reconstituted them with WT bone marrow, and infected them with *C. neoformans*. As expected, chimeric mice did not show a skewed Th2 response (Supplementary Fig. 3a). Of note, the inverse chimeras - irradiated WT mice reconstituted with *Dock8*$^{-/-}$ bone marrow cells - were not viable.

Having determined that the type-2 skew in *Dock8*$^{-/-}$ mice was driven by Dock8- deficiency in the hematopoietic compartment, we more thoroughly characterized the immune cell populations in the lung 20 days post-infection with *C. neoformans* (Fig. 3a; gating strategy shown in Supplementary Fig. 3b). As described (Fig. 1h), eosinophils were significantly increased in *Dock8*$^{-/-}$ mice with, on average, 10-fold higher numbers on day 20 post infection compared to WT mice (Fig. 3a). The increased eosinophil numbers were expected given the role for IL-5 in eosinophil tissue recruitment, and eosinophilia has also been described in DOCK8-deficient humans[7]. We also observed significantly higher numbers of DCs in the lungs of *Dock8*$^{-/-}$ mice, but all other immune cell subsets examined were similar between *Dock8*$^{-/-}$ and WT mice (Fig. 3a). To determine whether the Th2 bias in Dock8-deficiency was intrinsic to one of the immune cell types present, we generated mice with cell-specific deletions of Dock8 using the cre-lox system and infected them with *C. neoformans*, and investigated whether these conditional KO mice recapitulated the Th2 bias. We did not observe the biased Th2 CD4$^+$ T cell response, increased GMCSF production, or greater eosinophil recruitment at day 20 post infection when *Dock8*-floxed mice were crossed with Lck-cre (T cell specific), CD11c-cre (DCs, some macrophage subsets including alveolar macrophages, some activated T cells), LysM-cre (neutrophils, some macrophages), or eo-cre (eosinophils) (Fig. 3b and Supplementary Fig. 4a-c). Moreover, the depletion of B cells in *Dock8*$^{-/-}$ mice one day prior to infection using anti-CD20 did not abrogate the type-2 biased response (Supplementary Fig. 4d). Interestingly, in the T cell restricted KO (T-Dock8$^{-/-}$) mice, a significantly higher proportion of CD4$^+$ T cells produced IL-17 than in WT mice, suggesting that Dock8-deficient T cells were fully capable of differentiating into Th17 cells, and thus that the previously observed defect in IL-17 production in Dock8-deficiency is not T cell intrinsic (Supplementary Fig. 4c)[13, 41]. Of note, the absence of the Th2-biased response when Dock8-deficiency was restricted to T cells or CD11c$^+$ cells,

supported the notion that changes in T cell priming were likely not driving the type-2 T cell differentiation in *Dock8*$^{-/-}$ mice, despite the previously described abnormal globular morphology of *Dock8*$^{-/-}$ DCs[11]. Indeed, when WT T cells were transferred into *Dock8*$^{-/-}$ mice, we observed that the WT T cells behaved the same as endogenous *Dock8*$^{-/-}$ T cells with regard to their production of Th2 cytokines, IL-17, and TNFα, further corroborating that the signals leading to the Th2-biased response were T cell extrinsic (Fig. 3c,d).

An additional candidate immune cell population not quantified in Fig. 3a, but known to potentiate Th2 responses and able to produce IL-4, IL-5 and IL-13 early in a type 2 inflammatory process are group 2 innate lymphoid cells (ILC2)[42]. Dock8 was shown to be critical for the development and survival of ILC3s in the gut[16], but the role of Dock8 in lung ILCs generally, or in group 2 ILCs specifically, was unknown. To determine whether increased ILC2 activation was responsible for the Th2 bias in *Dock8*$^{-/-}$ mice, we examined ILC numbers at early and late points during infection. At both 4 and 20 days post-infection, ILCs were virtually absent in the lungs of *Dock8*$^{-/-}$ mice (Supplementary Fig. 4e,f). Moreover, we detected no selective increase in ILC2s following *C. neoformans* infection (Supplementary Fig. 4g,h). Thus, increased ILC2 responses were not driving the type-2 biased CD4^{+} T cell response in the Dock8$^{-/-}$ mice.

Based on previously published data[43], none of the conditional knockouts tested likely targeted all mononuclear phagocyte populations (MNP) observed in the lungs of WT and *Dock8*$^{-/-}$ mice after *C. neoformans* infection (Fig. 3a; gating strategy in Supplementary Fig. 3b). To be able to specifically target non-DC MNPs for deletion of *Dock8*, we first confirmed published data[44] that the fractalkine receptor CX3CR1 was highly expressed on non-DC MNPs, with intermediate expression by DCs and granulocytes, and no expression on lymphocytes in the lungs of WT and KO mice 20 days post infection with *C. neoformans* (Fig. 3e). To interrogate the potential role of non-DC MNPs in the Th2 bias in Dock8-deficient mice, we crossed *Dock8*-floxed mice with CX3CR1-ERT2-cre mice that we treated with tamoxifen (CX3CR1-Dock8$^{-/-}$) and infected with *C. neoformans* (Fig. 3f; *Dock8* knock-out efficiency shown in Supplementary Fig. 4i). Eight days post-infection, there was a similar expansion of activated CD4^{+} T cells in control, full Dock8 KO, and CX3CR1-Dock8$^{-/-}$ mice (Fig. 3g). In contrast to the other conditional KO strains tested, in CX3CR1-Dock8$^{-/-}$ mice, but not in any of our control mice, there was a Th2 bias comparable to full *Dock8*$^{-/-}$ mice (Fig. 3h). The GM-CSF response was not significantly different in CX3CR1-Dock8$^{-/-}$ mice from either WT or KO mice at this time point, being intermediate between WT and KO (Fig. 3h). Production of IL-17 or TNFα was not different between groups (Supplementary Fig. 4j).

Together these data pointed to non-DC MNPs as the cell population in which a lack of Dock8 expression was sufficient to result in the type-2 biased CD4^{+} T cell response.

Dock8$^{-/-}$ mononuclear phagocytes activate caspases and shatter while migrating

We next looked to identify how the loss of Dock8 in CX3CR1^{+} MNPs was altering CD4^{+} T effector differentiation during infection. Given that we previously showed that Dock8-deficient T cells undergo cytothripsis (migration-induced cell shattering) as they migrate through collagen-dense tissue[12], we measured the frequency of dead and dying cells in the

lung post infection. *Dock8*$^{-/-}$ mice had a significantly higher frequency of dead immune cells at both 8 and 20 days after *C. neoformans* infection than WT mice, and a slight but non-significant increase in frequency of apoptotic cells (Fig. 4a). Most AnnexinV^{+} cells had already downregulated lineage surface markers, making it difficult to determine in which cell types the death rate was increased in *Dock8*$^{-/-}$ mice. To investigate this, we measured the expression of cleaved caspase-3 (cc-3), a cysteine protease which in its cleaved form mediates processes downstream of the initiation of apoptosis[45, 46]. Expression of cc-3 varied between four key populations in WT mice: lymphocytes, granulocytes, DCs, and non-DC MNPs (Fig. 4b, c). Strikingly, in *Dock8*$^{-/-}$ mice we observed a significantly higher proportion of cc-3^{+} cells only in the non-DC MNP subset (Fig. 4b, c, gating strategy in Supplementary Fig. 3b). Notably, this increase in cc-3^{+} cells in non-DC MNPs was recapitulated in infected CX3CR1-Dock8$^{-/-}$ mice, indicating that caspase-3 activation in non-DC MNPs resulted from a cell-intrinsic loss of Dock8 (Fig. 4d).

We next asked whether the greater cell death and caspase-3 activation in non-DC MNPs in *Dock8*$^{-/-}$ mice could be a direct result of the role of Dock8 in maintaining cell cohesion during migration. To investigate this, we generated bone marrow-derived DCs (BMDCs) from *Dock8*$^{-/-}$ mice and WT mice expressing a GFP reporter for F-actin (LifeAct-GFP mice). In lieu of reliable *ex vivo* migration assays with primary MNPs other than DCs, BMDCs are a reasonable *in vitro* surrogate. Indeed, BMDCs constitute a heterogeneous population that shares many features with monocytes in particular[47]. We seeded BMDCs into standard density (1.7 mg/mL) collagen matrices and tracked their movement. Surprisingly, even at this lower collagen density, in which *Dock8*$^{-/-}$ T cells migrate normally and exhibit no morphological defects[12] (Supplementary Video 1, Supplementary Fig. 5a, b), the majority of *Dock8*$^{-/-}$ BMDCs became entangled and underwent cytothripsis over the course of a 3-hour migration assay as they moved, while WT BMDCs remained intact throughout (Fig. 4e and Supplementary Video 2). Cell death of *Dock8*$^{-/-}$ BMDCs was migration-dependent, as we observed a significant reduction in the viability of moving KO cells after 45 minutes, but not WT BMDCs, compared to cells kept in culture for the same period (Fig. 4f). Automated quantification of BMDC shape from 5 independent migration experiments showed that a stretched morphology in the absence of Dock8 was a consistent observation, with most *Dock8*$^{-/-}$ BMDCs strikingly elongated after 3 hours of migration, unlike WT BMDCs (Fig. 4g). Indeed, the cytothripsis of *Dock8*$^{-/-}$ BMDCs was evident by the blebbing of GFP and morphological distress observed at higher magnifications (Fig. 4h and Supplementary Video 3). Thus, our data suggested that *Dock8*$^{-/-}$ BMDCs, and by extension possibly MNPs *in vivo*, were exquisitely sensitive to migration-induced cell death – far more so than T cells.

Based on the increased activation of caspase-3 and immune cell death in *Dock8*$^{-/-}$ mice in the lung following *C. neoformans* infection, we next asked whether caspase activation played a role in the type-2 bias in *Dock8*$^{-/-}$ mice. To address this, we treated *Dock8*$^{-/-}$ mice with Q-VD-OPh, a potent and irreversible pan-caspase inhibitor[48], every other day during infection with *C. neoformans* and examined the CD4^{+} T cell cytokine response in the lungs of mice at 8 days post infection (Fig. 4i). Inhibition of caspase activation did not alter the expansion of CD44^{hi} CD4^{+} T cells (Fig. 4j), but it abolished the Th2 bias in treated *Dock8*$^{-/-}$ mice and significantly reduced GM-CSF production by CD4^{+} T cells (Fig.

4k), while production of IFNγ and TNFα increased significantly and IL-17 was unaffected (Supplementary Fig. 5c).

Thus, caspase activation in infected Dock8$^{-/-}$ mice, which was attributable to the migration-induced loss of cell cohesion and death of MNPs, was a critical driver in the Th2 bias in Dock8-deficiency.

IL-1β is a necessary but not sufficient driver of GM-CSF and Th2 cytokine production in Dock8-deficiency

Specific caspases play roles in initiating or executing apoptosis, but distinct caspases are inflammatory and trigger inflammasome activation[46]. Given the effect of the pan-caspase inhibitor in abrogating the Th2 skew in Dock8-deficiency, we wanted to more thoroughly characterize which caspases, in addition to caspase-3, were being activated during cytothripsis. We reasoned that determining the type of death program(s) implicated would shed light on the molecular mediators involved in driving the type-2 CD4$^+$ T cell response. To that end, we examined the activation of proteins involved in apoptosis (caspase-3 and caspase-8) and pyroptosis (caspase-1), as well as necroptosis (mixed lineage kinase domain-like protein, MLKL) in BMDCs that either migrated in a collagen matrix or remained in culture for the same time period. We found that migrating *Dock8*$^{-/-}$ BMDCs had increased expression of activated caspases 1, 3, and 8 after only 45 minutes of migration, which was absent in migrating WT BMDCs (Fig. 5a). In contrast, neither non-migrating WT nor *Dock8*$^{-/-}$ BMDCs expressed increased levels of activated caspases 1 and 3, and cleaved caspase 8 was not different between non-migrating KO compared to WT BMDCs (Fig. 5a). Additionally, expression of MLKL was similar between WT and *Dock8*$^{-/-}$ BMDCs, while expression of phosphorylated (active) MLKL was slightly higher in WT BMDCs after migration, suggesting that while migrating *Dock8*$^{-/-}$ cells were activating both apoptotic and pyroptotic caspases, cells were not dying by necroptosis, a caspase-independent form of cell death.

To confirm our results that the loss of cell cohesion *Dock8*$^{-/-}$ cells also led to the activation of the inflammatory caspase-1, which cleaves pro-IL-1β into its active form, we investigated whether the migration-induced shattering of *Dock8*$^{-/-}$ BMDCs resulted in the release of IL-1β. We repeated the BMDC 3D migration assays and measured IL-1β in the collected supernatant by ELISA. Indeed, while amounts were low, overall the migrating BMDCs released more IL-1β than non-migrating BMDCs, with a trend towards more IL-1β released by KO BMDCs (Fig. 5b). In parallel, we performed a bronchoalveolar lavage (BAL) 20 days after infection with *C. neoformans* and did a comprehensive screen of cytokines. Of a total of 31 cytokines measured, we found 14 cytokines that were significantly different in the BAL fluid (BALF) of *Dock8*$^{-/-}$ mice, including IL-1β, which was increased (Fig. 5c). Notably, BALF IL-4 and IL-13 levels were significantly higher while IL-5 levels were trending higher in *Dock8*$^{-/-}$ mice (Fig. 5c and Supplementary Fig. 5d), consistent with the Th2 bias we observed by examining CD4$^+$ T cell responses. Conversely, IL-17 was significantly decreased, again consistent with our CD4$^+$ T cell cytokine data (Fig. 5c and Fig. 2b). Interestingly, vascular endothelial growth factor (VEGF) was decreased, which has been shown to be inhibited by type-2 cytokines[49], and we also detected increased levels of

several chemokines, including CCL2, CXCL10 and CCL3 (Fig. 5c). Importantly, in addition to our data from the BALF, we also detected substantially greater IL-1β levels in total lung homogenate by ELISA (Fig. 5d).

To probe whether IL-1 was important in the development of the Th2-differentiation bias in Dock8-deficiency, we crossed *Dock8*$^{-/-}$ mice with mice lacking the IL-1 receptor (IL-1R$^{-/-}$) and infected them with *C. neoformans*. The absence of IL-1R signaling in *Dock8*$^{-/-}$ mice led to a significant decrease in the number of activated CD4^{+} T cells in double knockout mice compared to *Dock8*$^{-/-}$ mice, though not to WT levels (Fig. 5e), consistent with a previously described role for IL-1β in the expansion of effector CD4^{+} T cells[50]. Importantly, production of Th2 cytokines and GM-CSF was significantly reduced in *Dock8*$^{-/-}$ mice without IL-1R expression (Fig. 5f). IFNγ and TNFα production was also significantly decreased in double knockout mice compared to *Dock8*$^{-/-}$ mice, while IL-17 was unaltered (Supplementary Fig. 5e). Surprisingly, eosinophilia was significantly, but only slightly reduced in double knockout mice, despite the abrogated type-2 bias, suggesting that the increased type-2 cytokine levels may not entirely explain by itself the eosinophilia in DOCK8-mutant individuals (Fig. 5g).

Our data suggested that IL-1 was playing a critical role in the altered CD4^{+} T cell responses in the absence of Dock8, but did not address whether IL-1 was acting through an intermediate population or acting directly on CD4^{+} T cells. To investigate whether IL-1R signaling in CD4^{+} T cells was necessary for the observed type-2 differentiation bias, we crossed *Dock8*$^{-/-}$ mice with T cell deficient (TCRβ$^{-/-}$) mice and then transferred IL-1R$^{-/-}$ T cells into both TCRβ$^{-/-}$ and Dock8/TCRβ dKO mice to generate either WT or *Dock8*$^{-/-}$ mice with only T cells selectively lacking IL-1R expression (Fig. 5h). We used WT T cells, as we had previously shown that Dock8-deficiency in T cells was not required for the Th2-biased response (Fig. 3b,d). We allowed the transferred T cells to reconstitute the *TCR*β$^{-/-}$ recipients for 8 weeks before infecting the mice with *C. neoformans*. As in the full IL-1R KO, the absence of IL-1R signaling on CD4^{+} T cells led to their decreased expansion (Fig. 5i), irrespective of whether the *TCR*β$^{-/-}$ recipients were Dock8 KO or WT. Importantly, when the lack of IL-1R expression was restricted to T cells, this abolished the Th2 bias, decreased GM-CSF production and normalized the eosinophil counts in the *TCR*β$^{-/-}$ *Dock8*$^{-/-}$ recipients as compared to the *TCR*β$^{-/-}$ recipients (Fig. 5j, k). IL-17 production was significantly increased in both *TCR*β$^{-/-}$ WT and *Dock8*$^{-/-}$ recipients, as compared to the *Dock8*$^{-/-}$ with normal IL-1R expression on T cells, while TNFα production by CD4^{+} T cells remained elevated even in the absence of IL-1R expression (Supplementary Fig. 5f).

Given our data on the importance of IL-1R signaling in the Th2-biased response, we wanted to determine whether the pan-caspase inhibition abolished the Th2 bias entirely through the prevention of caspase-1 activation and release of IL-1β. To do so, we blocked caspase activation in *C. neoformans* infected *Dock8*$^{-/-}$ mice using Q-VD-Oph treatment on its own as before (Fig. 4i-k), or in combination with the addition of exogenous IL-1β (Fig. 5l). Interestingly, adding back IL-1β during Q-VD-Oph treatment did not restore the Th2 bias (Fig. 5l). Addition of exogenous IL-1β also did not increase GM-CSF production in treated

Dock8$^{-/-}$ mice, but it led to significantly increased TNFα production compared to untreated WT mice (Supplementary Fig. 5g).

Thus, our data show that IL-1 signaling on T cells drives the Th2 bias in Dock8-deficiency, but that IL-1β alone, while a necessary signal, is not sufficient to induce the type-2 skew in the absence of caspase activation.

GM-CSF plays an amplifying role in the Th2 skew in Dock8-deficiency

Previous work demonstrated that IL-1 is an important signal in driving GM-CSF production by epithelial cells in asthma and type 3 ILCs in intestinal homeostasis[51, 52]. Interestingly, the production of GM-CSF by CD4$^+$ T cells has thus far been primarily shown in the context of experimental autoimmune encephalitis (EAE), where IL-1 plays a critical role in driving GM-CSF production by Th17 cells[53]. Unlike in EAE, we observed that the increased GM-CSF production by CD4$^+$ T cells, which was consistently increased in *Dock8*$^{-/-}$ mice across different infection models (Fig. 2a), tracked primarily with type-2-cytokine producing helper T cells (Fig. 6a). We found that in both *C. neoformans* and influenza A infection, although not in CFA immunization, the overall increase in GM-CSF production by CD4$^+$ T cells in *Dock8*$^{-/-}$ mice was largely attributable to Th2 cells (Fig. 6b). While consistent with the elevated IL-1β levels and the role for IL-1 in stimulating GM-CSF, this observation was surprising, given that GM-CSF production had not previously been described to track with Th2 cells. Of note, the increased level of GM-CSF in the lung was consistent with the reduced fungal burden in *Dock8*$^{-/-}$ mice despite the Th2-biased response (Fig. 1f), given the role for GM-CSF in control of *Cryptococcus* infections in both humans and mice[54, 55, 56, 57, 58].

We next tested the hypothesis that there was a (direct or indirect) role for GM-CSF in the Th2 biased response in *Dock8*$^{-/-}$ mice during infection. To determine whether GM-CSF was an important signal in the Th2-differentiation in the lung, rather than being required during CD4$^+$ T cell activation, we treated *Dock8*$^{-/-}$ mice with a neutralizing antibody against GM-CSF from 8 days post-infection every other day (Fig. 6c). Treatment with αGM-CSF slightly decreased the expansion of activated CD4+ T cells in *Dock8*$^{-/-}$ mice (Fig. 6d). Unexpectedly, we observed a significant decrease in the frequency of Th2 cells in the lungs of αGM-CSF treated *Dock8*$^{-/-}$ mice, although Th2 frequencies remained slightly greater than in WT mice (Fig. 6e). In contrast, blocking GM-CSF did not impact TNFα, IL-17, or IFNγ production (Supplementary Fig. 6a). Interestingly, αGM-CSF treatment also greatly reduced the frequency of GM-CSF-producing CD4$^+$ T cells (but not down to WT levels), suggesting that GM-CSF was amplifying its own production (Fig. 6e). Eosinophilia was also significantly reduced in αGM-CSF treated mice (Fig. 6f), in line with the decrease in the type-2 bias we observed.

It was unlikely that GM-CSF was acting in an autocrine manner, as we did not detect the GM-CSF receptor (CD116) on CD4$^+$ T cells (Supplementary Fig. 6b), consistent with previous data[59]. Unlike published data from rat or human epithelial cells, we also did not detect CD116 expression on mouse lung epithelial cells (Supplementary Fig. 6b) suggesting it was not acting via epithelial induction of alarmins either. Given that lack of Dock8 specifically in MNPs was important in driving the Th2-biased response, we asked whether

GM-CSF could amplify Th2 cytokine production by acting on MNPs. Indeed, we observed that non-DC MNPs in particular highly expressed the GM-CSF receptor (Supplementary Fig. 6c). This was important for MNP function, as we found that when we cultured WT monocytes isolated from the bone marrow with GM-CSF and LPS, either alone or in combination, expression of pro-IL-1β was markedly increased only when both GM-CSF and LPS were added together (Fig. 6h). This is in line with previous findings that GM-CSF signalling in the presence of LPS increased production of pro-IL-1β by DCs and macrophages[60].

Collectively, our data suggested that GM-CSF was playing a role in amplifying in the Th2 skew in Dock8-deficiency, at least in part through increasing IL-1β production.

Cell death provides a necessary and sufficient type-2-inducing signal

We identified caspase-dependent cell death as a critical driver of the Th2 biased $CD4^+$ T cell response in Dock8-deficiency with IL-1β being a necessary, but not sufficient, stimuli downstream of caspase activation (Fig. 5l). Therefore, we wanted to understand whether cell death could act as a type-2 differentiation signal more generally, even in WT mice with no impaired cell migration. In the same setting, we wanted to confirm that IL-1β on its own was not sufficient to lead to a type-2 skewed response. To test this, we infected WT ($CD45.2^+$) mice with *C. neoformans* and treated them either with irradiated $CD45.1^+$ thymocytes, IL-1β, or PBS daily from day 4 post infection (Fig. 7a). We injected the irradiated thymocytes intravenously, reasoning that it would lead to many of the thymocytes being trapped in the lung vasculature, perhaps allowing them to extravasate and enter the lung parenchyma in which $CD4^+$ T cell responses were taking place. There was no difference in expansion of activated $CD4^+$ T cells among the groups (Fig. 7b). Strikingly, however, on day 8 post infection, mice that received irradiated cells had a significantly higher frequency of $CD4^+$ T cells producing IL-4, IL-5 or IL-13 in the lung, while mice that received only IL-1β did not show an increased Th2 response compared to control mice (Fig. 7c). Mice receiving either irradiated cells or IL-1β had a significant increase in the frequency of GM-CSF producing $CD4^+$ T cells – to a greater extent in mice receiving IL-1β (Fig. 7c). Only mice that received IL-1β had an increase in TNFα and IL-17 production (Fig. 7c). Eosinophil infiltration was similar among all groups, as we had also observed on day 8 in *Dock8*$^{-/-}$ mice, generally arriving in increased numbers after this time point (Fig. 7d). Notably, measurements of IL-1β in lung homogenate corroborated that the administration of irradiated cells also led to an increase in IL-1β, albeit not to the levels detected in the group treated with exogenous IL-1β (Fig. 7e).

Together, our data suggests that caspase-dependent cell death can act as a signal inducing the production of type-2 cytokines by $CD4^+$ T cells and is consistent with the idea that while IL-1β is not sufficient on its own to drive a type-2 response, it is a necessary component of the signal provided by cell death.

Discussion

Individuals with inherited defects in DOCK8 expression are prone to allergic, type-2 $CD4^+$ T cell responses, but why this is the case has been unclear[7, 13]. Our data show that *Dock8*$^{-/-}$

MNPs are exquisitely sensitive to cell death as they migrate through 3D tissue, shattering as they do so and activating caspase-1 and -3. We link dysregulated MNP migration to the release of IL-1β, and restricting Dock8-deficiency to non-DC MNPs, which express high levels of the fractalkine receptor CX3CR1, recapitulates the Th2 bias in *Dock8*$^{-/-}$ mice *in vivo*. In the setting of pulmonary *Cryptococcus* and influenza A virus infection, or of subcutaneous CFA immunization, we show that in Dock8-deficient mice, IL-1β acts on CD4^{+} T cells to induce the production of GM-CSF and drives the type-2 differentiation of recruited effector CD4^{+} T cells (Supplementary Fig. 7). Consistent with Dock8-deficiency introducing signals that divert a normally non-Th2 stimulus to one eliciting type-2 cytokine production by CD4^{+} T cells, we did not see an exacerbated type-2 response in the context of the strong Th2-inducing stimulus provided by helminth infection. Thus, Dock8 expression is necessary to prevent inappropriate skewing of the CD4^{+} T cell response, but it does not directly regulate induced Th2 responses. The type-2 CD4^{+} T cell differentiation bias observed in the absence of Dock8 is abrogated by blocking IL-1R signalling or upon treatment with a broad-spectrum caspase inhibitor, and does not require Dock8-deficiency in T cells or DCs. Moreover, treatment with anti-GM-CSF greatly reduces the Th2 response, resulting in a reduction in IL-1β production. Importantly, we implicate cell death as a type-2 differentiation signal even in WT mice with normal Dock8 expression.

The cytoskeletal processes involved in the dysregulated migration of *Dock8*$^{-/-}$ cells remain incompletely understood. It is therefore unclear why the migration of T cells in less constraining tissue environments is largely unaffected and in dense tissue T cell shattering is a rare event, while MNPs struggle to traverse even low-density collagen matrices. Janssen *et al* described direct binding of DOCK8 to the WASP-interacting protein (WIP), suggesting that DOCK8 regulates F-actin assembly[21]. However, we have previously shown that loss of WASP expression in migrating T cells did not lead to the same cell elongation and shattering as did loss of DOCK8[12]. Instead, our data suggested that DOCK8 was acting via PAK1/2 to result in the discoordination of cell movement impacting both F-actin and microtubule positioning[12]. Moreover, recent data from the Sixt lab has implicated microtubules and the positioning of the microtubule-organizing centre in cellular direction choice[61]. Regardless, it is intriguing that the severity of the effect of the lack of DOCK8 on the integrity of immune cell cytoskeletal processes appears to be cell type-dependent and will be the subject of future investigations.

Unexpectedly, given the important pro-inflammatory role of IL-1 in many contexts[62], we demonstrated that IL-1β is a necessary signal in the Th2 bias observed in *Dock8*$^{-/-}$ mice. Previous work showed that treatment with IL-1β augmented the expansion of all antigen-specific CD4^{+} T cells[50]. Moreover, IL-1β has been primarily implicated in driving the production of IL-17 by CD4^{+} T cells, especially in pre-clinical models of inflammatory bowel disease or neuro-inflammatory diseases such as multiple sclerosis or arthritis[63, 64] However, administration of IL-1β has also been shown to enhance IgE production and the frequency of IL-4 producing CD4^{+} T cells upon OVA + LPS stimulation *in vivo*[50]. Of note, in Dock8-deficient mice we showed that the Th2 response tracked with an increased production of GM-CSF. Consistent with our experiments showing that the absence of IL-1R on T cells abrogates this increased GM-CSF response, IL-1R signaling has been shown to be important in driving GM-CSF production in pathogenic IL-17 producing CD4^{+} T cells

in EAE[65, 66]. Whether the signals that lead to GM-CSF production by Th17 and Th1 cells, are the same as those for Th2 cells needs to be determined. Of note, IL-1β also induces production of GM-CSF by group 3 ILCs in the gut[52], suggesting that an IL-1β-GM-CSF cytokine circuit might be conserved across multiple cell types.

Interestingly, constitutive expression of GM-CSF by $CD4^+$ T cells was recently shown to be sufficient to drive the expansion of moDCs and lead to CNS inflammation[67]. Indeed, given the high expression of the GM-CSF receptor by MNPs, previous data from autoimmune diseases that activated MNPs are recruited by GM-CSF, and our data and that of others that GM-CSF leads to the release of greater amounts of IL-1β by MNPs[68], suggests that a positive feedback loop between IL-1β and GM-CSF may play a role in Dock8-deficiency. Thus, GM-CSF, which enhances pro-IL-1β production, leads to increased numbers of MNPs in the lung that are prone to migration-induced shattering and amplifies production of IL-1β. Given this amplification, treating DOCK8-deficient humans with an IL-1R antagonist, such as Anakinra, may be beneficial in abrogating symptoms in those with severe allergies. Moreover, the presence of residual DOCK8-mutant MNPs in patients after bone marrow transplant might explain the continued presence of allergic disease, in addition to long-lived anti-allergen IgE[69].

Whether GM-CSF plays a role in Th2 responses beyond increasing IL-1β production remains unclear. While GM-CSF production by $CD4^+$ T cells has not previously been shown to play a role in Th2 responses, GM-CSF production by airway epithelial cells has been associated with allergic disease. Earlier studies established that antibody blockade of GM-CSF diminished Th2-cytokine production and ameliorated airway hyperresponsiveness induced by environmental pollutants or allergens[70, 71]. In addition, airway expression of GM-CSF promoted allergic sensitization to OVA, resulting in eosinophil recruitment and type-2 cytokine production[72]. More recently, airway epithelial cell production of GM-CSF was shown to lead to Th2 responses in a house dust mite asthma model, but this was induced by IL-1α release from epithelial cells acting in an autocrine manner and not on antigen-specific $CD4^+$ T cells directly[51]. Together, our data and that of others provides evidence that an IL-1β-GM-CSF cytokine axis may be an important signal leading to Th2 cytokine production.

Our observation that the shattering of *Dock8*$^{-/-}$ immune cells was the cause of the distinct cytokine response in Dock8-deficient mice during *C. neoformans* infection led to us investigate whether increased cell death might, even in WT mice, result in greater Th2 responses. Many of the diverse stimuli of Th2 responses are known to cause substantial cell death, such as animal-derived venoms[73], infection with metazoan parasites[74], or environmental irritants[75]. Moreover, the role of cell death in type-2 responses is implicit in the paradigm of Th2 immunity as a wound repair response[74]. Indeed, recent work has shown that apoptotic cell sensing is required in conjunction with IL-4 or IL-13 to initiate a tissue repair program in macrophages[76]. Moreover, commensal-specific Th17 cells in the skin have been shown to produce IL-5 and IL-13 upon tissue injury[77]. In addition, the failure of epithelial cells to efferocytose dying cells in an asthma model led to exacerbated type-2 cytokine production, increased eosinophil recruitment, and greater airway inflammation[78]. Here we show that in the context of pulmonary *C. neoformans* infection, the addition of

apoptotic cells was sufficient to increase the frequency of type-2 cytokine producing $CD4^+$ T cells in the lung. As observed in Dock8-deficiency, IL-1β was a necessary but not sufficient signal downstream of cell death leading to type-2 responses. Our data do not directly address whether it is apoptosis or pyroptosis that is the key trigger, given that we found that migrating Dock8-deficient MNPs activated both pathways. Moreover, it is possible that the high number of apoptotic cells we transferred into WT mice during infection overwhelmed the capacity of lung cells to efficiently remove them, and it has been previously shown that irradiated cells, if not cleared, can subsequently release damage-associated molecular patterns (DAMPs) and thus lead to IL-1β production[79]. Importantly, we show that cell death and caspase activation is a key Th2-driving signal that is not replicated by IL-1β on its own. What this signal is remains to be determined. Recent work by Ravichandran's group has identified dozens of metabolites secreted by apoptotic lymphocytes and macrophages[80]. It will be interesting to investigate whether any of these could, together with IL-1β, elicit type-2 immunity.

It is tempting to speculate that, in addition to changes in our exposure to pathogens postulated by the hygiene hypothesis[81], an important contributor to the global rise in allergies is our increased exposure to chemicals and pollutants capable of inducing cell death and IL-1β release, thus establishing a bias in $CD4^+$ T cell responses. Overall, our work suggests that blocking specific cytokine signals resulting from increased cell death, such as IL-1β and GM-CSF, could be beneficial in settings of allergic responses where type-2 $CD4^+$ T cells are critical drivers of disease. This work also emphasizes the unique opportunity provided by rare inherited immunodeficiencies to study perturbations in immune function as a means to gaining insight into the complex equilibrium established to prevent disease while protecting from infection.

Materials and Methods

Human samples

Whole blood samples were obtained from individuals who had provided written informed consent to participate in research protocols approved by the National Institutes of Health (NIH) Institutional Review Boards. Peripheral blood mononuclear cells (PBMCs) were enriched from whole blood using Ficoll-Paque PLUS (GE Healthcare) gradient density centrifugation, and pan T cells were isolated by negative selection (Miltenyi). Cells were restimulated with 10ng/mL PMA and 500ng/mL ionomycin (Calbiochem) at 37°C for 2 hours followed by treatment with GolgiPlug (BD Biosciences) at 1:1,000 for an additional 6 hours. Extracellular stains were performed for 20 minutes at 4°C followed by fixation and permeabilization with BD Cytofix/Cytoperm Kit. Cells were resuspended in perm/wash buffer containing intracellular antibodies and stained for 1 hour at 4°C. Directly conjugated antibodies were used as follows: CD45RO (clone UCHL1), CD2 (clone RPA-1.10), IL-13 (clone JES10-5A2), and IL-4 (clone MP4-25D2). Data were acquired on an LSRFortessa (BD Bioscience) and analysed using FlowJo software (Tree Star).

Mice

Dock8$^{-/-}$ and Dock8-floxed mice were generated by genOway (Lyon, France). In brief, two *lox*P sites were inserted flanking exons 9 and 10 of the *DOCK8* gene using neomycin selection cassette. To generate the pure knockout, highly chimeric males were mated with Cre deleter females. The presence of *lox*P sites in the Dock8-floxed mice and gene excision in the Dock8$^{-/-}$ mice was confirmed by PCR genotyping. Wild type C57BL/6 mice, CD45.1 congenic B6, CD11c-cre[82], Lck-cre[83], IL-1R$^{-/-}$ [84], CX3CR1-creER[85], and TCRβ$^{-/-}$ mice[86] mice were purchased from Jackson Laboratories (Bar Harbor, ME) and bred in-house. LysM-cre[87] mice were shared by Danielle Malo (McGill). The Eo-cre (eosinophil-specific cre) mice[88] were provided by James Lee (Mayo Clinic), and the LifeAct-GFP mice[89] were shared by Janis Burkhardt (U Penn). All mice in this study were on a B6 background and used for experiments at 8-12 weeks of age. Animal housing, care and research were in accordance with the Guide for the Care and Use of Laboratory animals and all procedures performed were approved by the McGill University Facility and the NIAID Animal Care Committee.

Infection and immunization models

Cryptococcus neoformans: H99 strain was initially obtained from Kyung Kwon-Chung, NIH, and frozen stocks (−80°C) prepared by loading fresh cultures from a YPD agar plate into 15% glycerol. Three days prior to infection, *C. neoformans* was streaked onto a YPD agar plate and on the day before infection, a single colony was inoculated in YPD broth and incubated for 12-16 hours at 30°C with agitation. Immediately prior to infection, *C. neoformans* was resuspended in cold PBS, mice were anesthetized with isofluorane and infected by intrapharyngeal aspiration with 5,000 CFU (or 50,000 CFU for survival experiments) in 20μl of PBS. Mice were euthanized and tissue was harvested 20 days post infection (unless otherwise specified). In survival experiments, mice were monitored daily from day 20 and euthanized when exhibiting signs of irreversible disease or a weight loss greater than 20% of original body weight.

Influenza A virus: PR/8 strain was kindly shared by Silvia Vidal (McGill). Mice were anesthetized as described above and infected intranasally with either 400 or 2,000 PFU of the PR/8 strain of influenza A virus in PBS. Mice were euthanized and tissue was harvested 7 days post-infection. Quantitative RT-PCR was used to determine the viral loads as described[90].

Heligmosomoides polygyrus: Mice were infected orally via gavage with 200 *H. polygyrus* L3 larvae in 200uL of cold PBS. Mesenteric (gut-draining) lymph nodes were harvested 7 days post-infection.

Complete Freund's Adjuvant (CFA): Inactivated *Mycobacterium tuburculosis* (Mtb) (5mg/mL) was added to CFA and combined 1:1 with OVA peptide (200ug/mL) in PBS. The mixture was emulsified by 20 minutes on ice immediately prior to subcutaneous injection of 25uL in the rear flank of each mouse.

Leukocyte isolation

Where specified, intravascular staining using 2.5μg α-CD45-FITC or APC was performed as previously described[40] prior to euthanasia and tissue harvest. Infected lungs were harvested into cold PBS and minced with scissors before being incubated in digestion buffer (1mg/mL collagenase D, 50U/mL DNAse I, 1mg/mL hyaluronidase, 1% L-glutamine, and 1% pen/strep in RPMI) at 37°C with agitation for 30 min. Tissue was passed through a 100μM filter with 1% FCS in PBS and resuspended in 10mL of 37% Percoll in RPMI and centrifuged at 2000rpm at 22°C for 20 minutes. RBC lysis buffer was added for 3 min, samples refiltered and resuspended in complete RPMI. Draining (mediastinal) and non-draining (brachial and inguinal) lymph nodes were harvested into cold 1% RPMI and passed through a 70μM filter with 1% RPMI. Cell counts were determined by diluting single cell suspension 1:10 in Trypan blue and manually counting live (Trypan blue negative) single cells on a hemacytometer.

Mouse T cell and myeloid cell *in vitro* restimulation and flow cytometry

For intracellular cytokine detection in T cells, single cell suspensions of lung cells were stimulated with α-CD3 and α-CD28 (Invitrogen; both at 2μg/mL) in 96-well plates in the presence of brefeldin (BFA) and monensin (Invitrogen; both diluted 500x) for 5 hours at 37°C. For intracellular cytokine detection in myeloid cells a protocol previously published[91] was modified for *C. neoformans* infection and lung cells were stimulated with 50,000 CFU of *C. neoformans* for 5 hours at 37°C with BFA/monensin. Samples were then incubated in Fixable Viability Dye (eBioscience) diluted in PBS for 20 minutes at 4°C. Extracellular antibodies were diluted in FACS buffer (2% FCS and 5mM EDTA in PBS) with Fc block (eBioscience) and incubated for 30 minutes at 4°C. Samples requiring intracellular staining were incubated in FoxP3 Transcription Factor Fixation/Permeabilization Concentrate and Diluent (Life Technologies) for 30 minutes at 4°C. Intracellular antibodies were diluted in permeabilization wash buffer and incubated as above. Directly conjugated antibodies used were as follows: Bcl6 (clone K1112-91), TCRβ (clone H57-597), CD5 (clone 53-7.3), CD64 (clone X54-5/7.1), siglecF (clone E50-2440), F4/80 (T45-2342) from BD Biosciences; CD11c (clone N418), CD45 (clone 30F11), CD127 (clone SB/199), CXCR5-biotin (clone SPRCL5), RoRγt (clone B2D), Ly6c (clone HK1.4), MHC-II (clone M5/114.15.2), GM-CSF (clone MP1-22E9), IL-4 (clone 11B11), IL-13 (clone eBio13A), IL-1α (ALF-161), pro-IL-1β (NJTEN3) from eBioscience; B220 (clone RA3-B62), CD11b (clone M1/70), CD4 (clone RM4.5), CD68 (clone FA-11), CD8 (clone 53-6.7), CD90.2 (clone 53-2.1), FoxP3 (clone FJK-16s), GATA3 (clone 16E10A23), T-bet (clone 4B10), Ly6G (clone 1A8), PD-1 (clone 29F.1A12), IL-5 (clone TRFK5), IL-17 (TC11-18H10.1), IFNγ (XMG1.2) from Biolegend; cleaved caspase-3 (clone 269518) and GM-CSFR (clone 698423) from R&D Bio. Data were acquired on an LSRFortessa (BD Bioscience) and analysed using FlowJo software (Tree Star). Boolean gating analyses to group cells according to all possible combinations of cytokines produced were performed using FlowJo.

Tissue fixation

Organs were fixed as described[92], incubated overnight, then washed twice, transferred to 30% sucrose, and allowed to sink for 4-6 hours. Tissue was mounted in O.C.T.

(Fisher Scientific) and stored at −80°C. Fixed tissue was cryosectioned at a thickness between 4-14μM for either hematoxylin and eosin staining or mucicarmine staining (McGill Histology Core).

Pharmacological treatments and cell transfers

Adoptive transfers: For DOCK8$^{-/-}$/TCRβ$^{-/-}$ recipients: spleen and inguinal, axillary, brachial, cervical, and mesenteric lymph nodes were harvested from IL-1R$^{-/-}$ mice into cold 1% RPMI and passed through a 70μM filter. RBCs were lysed and the cell suspension was enriched for T cells (StemCell EasySep T Cell Isolation Kit). For WT cells transferred into DOCK8$^{-/-}$ mice: spleens were harvested and processed as described above. Cells were stained for CD4, CD8, and CD5 and analyzed by flow cytometry. Total splenocytes were resuspended in cold PBS such that 1x10^7 T cells in 300μL were injected intravenously.

GM-CSF blockade: Beginning 8 days after infection with *C. neoformans*, mice were injected i.p. with 400μg of α-GM-CSF in 300μL PBS (hybridoma purified by BioXCell) or with an IgG isotype antibody in 300μL PBS or 300μL PBS alone.

Q-VD-OPh: 5mg of Q-VD-OPh (Cayman Chemical) was reconstituted in 1mL of DMSO and stored at −20C until use. Mice were injected i.p. with 3mg/kg of Q-VD-OPh in 300mL of ice-cold PBS or PBS alone beginning 1 day post-infection and every other day until the endpoint at 8 days post-infection.

Irradiated cell transfer: Thymocytes were harvested from congenically distinct wild type mice and passed through a 70μM filter in ice-cold PBS. Cells were irradiated at 4Gy immediately prior to transfer (1 x 10^7 cells/mouse in 300mL ice-cold PBS), and transferred i.v. on days 4, 5, 6, and 7 post-infection.

Tamoxifen treatment: Mice were orally gavaged with 5mg of Tamoxifen (Sigma) dissolved in corn oil and ethanol (9:1 ratio) for three consecutive days. A week following the first treatment, mice were infected and orally gavaged again with 5mg of Tamoxifen at days 1, 3, 5, and 7 post-infection.

B cell depletion: One day prior to infection with *C. neoformans*, mice were injected intravenously with 250ug Ultra-LEAF α-CD20 (Biolegend). Depletion of B cells was confirmed by flow cytometry of recruited lung cells.

Administration of exogenous IL-1β.—Mice were anesthetized with isofluorane and intrapharyngeally administered 50pg of rIL-1β (Biolegend) in 20uL of cold PBS on days 1, 3, 5, and 7 post-infection for the caspase-block experiments, or days 4, 5, 6, and 7 for the experiments involving transfer of irradiated thymocytes.

Cytokine assays

Bronchoalveolar lavage: On day 20 after infection with *C. neoformans*, mice were euthanized with CO_2 only and their lungs and trachea were surgically exposed. A 20g catheter was inserted into the trachea and lungs were flushed three times with 500μL of

PBS. Bronchoalveolar lavage fluid was spun down, the supernatant removed and stored at −80°C. Samples were shipped on dry ice to Eve Technologies (Calgary, Canada) and a Mouse Cytokine Array/ Chemokine Array 31-Plex Assay was performed.

Whole lung ELISA: Lung tissue was collected added to 1mL of PBS in Lysing Matrix D tissue homogenization tubes (MP Biomedicals) and homogenized at 6,000rpm for 40 sec in a Roche MagNA Lyzer. IL-1β was detected with the R&D mouse IL-1β DuoSet ELISA kit, and IL-12p70 was detected with the R&D mouse IL-12p70 DuoSet ELISA kit.

Monocyte culture: Bone marrow was harvested from the femurs of WT mice by flushing marrow from bones with cold 1% RPMI. Cells were incubated in RBC lysis buffer and monocytes were isolated from single cell suspension using the StemCell EasySep Mouse Monocyte Isolation Kit. Cells were incubated in complete media supplemented with 20ng/mL of recombinant murine GM-CSF at a concentration of $1.7x10^6$ cells/mL (Peprotech) for 24 hours, followed by intracellular staining for pro-IL-1β using flow cytometry.

RNA extraction and quantitative real-time RT-PCR

To assess the knock-down efficiency of *Dock8* in the T-Dock8$^{-/-}$ and CD11c- Dock8$^{-/-}$ we isolated T cells from lymph nodes and DCs from the spleen from both strains. Lymph node tissue was crushed through 70μM filters, and T cells were isolated as described above. For DC isolations, spleens were injected with 4mL of digestion buffer (RPMI supplemented with L-glutamine, penicillin-streptomycin, and 1mg/mL of collagenase II), incubated at 37°C for 15min, minced and incubated again at 37°C for 20 minutes. DCs were isolated using Mouse CD11c MicroBeads UltraPure (Miltenyi Biotec). To assess the knock-down efficiency of *Dock8* in the tamoxifen-treated CX3CR1- Dock8$^{-/-}$ mice, we isolated monocytes from bone marrow one week after the first three consecutive treatments with 5mg of Tamoxifen (described above). RNA was extracted using the TRIzol Plus RNA Purification Kit (Applied Biosystems). For Dock8 and GAPDH expression, previously published primers were used[93].

Bone marrow chimeras

Bone marrow was harvested from the femurs, tibias, and humeri of donor mice by flushing marrow from bones with cold 1% RPMI, passing cells through a 70μM filter, incubating in RBC lysis buffer, and then resuspending cells in PBS for injection. Two days prior to bone marrow transfer, recipient mice were put on neomycin water (2g/L) and kept on antibiotic water for 2 weeks following transfer. Recipients were irradiated twice (550 rads) 3 hours apart and reconstituted i.v. with $5x10^6$ donor cells within 8 hours.

Collagen Gel Migration Assay

BMDCs were generated as described by Sixt[94]. For all assays, mature BMDCs were stimulated with 200ng of lipopolysaccharide (LPS) for 12-20 hours prior to use. 3D collagen migration assays were performed using a custom-fabricated device consisting of a #1.5 coverslip, a glass microscope slide and a machined polycarbonate spacer of 1.2 mm thickness (modified from[94]). Bovine collagen solution (PureCol 3mg/mL, or Nutragen 6mg/mL, Advanced BioMatrix) was mixed with 10X DMEM and sodium bicarbonate

(Millipore Sigma) to a collagen concentration of 2.5 mg/mL or 4.8 mg/mL. Activated Lifeact-GFP T cells or Lifeact-GFP BMDCs in media (~$3x10^6$ cells/mL) were mixed with the collagen solution, resulting in a final collagen concentration of 1.7 mg/mL or 3.6 mg/mL. The collagen gel matrix containing the cells was polymerized at 37°C for 20 mins before CCL19 (1μg/mL, 20μL) was laid on top of the collagen-cell mixture. The diluted chemokine was allowed to diffuse into the gel for a further 20 min at 37°C to form a chemotactic gradient. For movies and cell shape analyses, T cells were visualized for at least 1 h (60 consecutive time points) and BMDCs were visualized for at least 3 h (180 consecutive time points) by a Zeiss 880 LSM with a N-Achroplan 10X/ NA 0.25 air objective or a 20x/ NA 1.0 water immersion objective (Carl Zeiss Canada Ltd.), where GFP was excited by the 488 nm Argon laser. Cells were maintained at 37°C for the duration of imaging by a heated platform surrounding the microscope. For ELISAs and western blots of migrating BMDCs, cells were allowed to migrate for either 3 hours (IL-1β quantification) or 45 minutes (activated caspase Western blot and flow cytometry viability staining), and then collagen gels were transferred to 1.7mL Eppendorf tubes and chopped roughly with scissors. Equal volume of Collagenase D was added to the tubes, which were put on a shaker at 37°C for 45 minutes. Tubes were then centrifuged at 3,500rpm for 7 minutes at 4°C. For ELISA, supernatants were transferred to fresh tubes at stored at −20°C until analysis. For Western blot, cell pellets were resuspended in Laemmli buffer and stored at −20°C until used. IL-1β was detected with the Abcam Mouse IL-1β SimpleStep ELISA kit. Standard curves were calculated according to manufacturer's instructions. For flow cytometry, cells were recovered from collagen matrices as described above and incubated in fixable viability dye (eBioscience) diluted in PBS for 20 minutes at 4°C.

Cell Shape Analysis

Cell shapes were quantitatively analyzed in two dimensions using a custom MATLAB App to extract the area, perimeter, major axis length, and minor axis length of each cell. Briefly, the original Zeiss lsm file consisting of a time series of 3D image stacks was loaded into the App and the image series was processed into a 2D maximum projection for a user selected set of lateral image planes at a specified time point. Image segmentation using the Canny edge detection method (using the MATLAB function *edge*) was performed, followed by morphological dilation of the subsequent binary mask (MATLAB function *imdilate*) to obtain cell outlines. The outline was then filled using morphological reconstruction (MATLAB function *imfill*) to obtain a final binary mask of all cells in the image. Quantitative cell shape parameters, specifically area, perimeter, major/minor axis length, were measured using the MATLAB function *regionprops*, and exported as a MS excel file.

Western Blot

Lysates were boiled for 5 minutes at 95 °C and an aliquot was resolved by SDS-PAGE and transferred to nitrocellulose by wet transfer in 10-20% methanol Tris-Glycine transfer buffer. Membranes were stained with Ponceau S Red before being dried and blocked with either 5% BSA or 5% non-fat dry milk in TBS + 0.1% Tween-20 (TBS-T) for 1 hour at room temperature. Membranes were incubated with primary antibody overnight at 4°C, washed 3 x 10 minutes with 0.1% TBS-T and secondary antibody was added for 1 hour at room temperature. Following another round of washes, proteins were visualized using enhanced

chemilumescence. Antibodies were used as follows: caspase-1 (total and p20), 1:1000 (Genentech, acquired through MTA); caspase-8 (cleaved, p41/43), 1:1000 (Cell Signaling #CST8592); caspase-3 (total), 1:750 (Cell Signaling #CST9662); phospho-MLKL (Ser345), 1:1000 (Abcam #ab196436); MLKL (total), 1:2000 (Abcam #ab172868); GAPDH, 1:3000 (Sigma #G8795).

Statistics

Data was analyzed by *t*-tests or Mann-Whitney tests, in the case of non-parametric data; Kruskal-Wallis analyis of variance (ANOVA) in the case of comparison between more than two groups (GraphPad Prism Software). The cutoff for significance was $P < 0.05$ for all analyses. Boolean gating analyses to group cells according to all possible combinations of cytokines produced were performed using FlowJo and R Project Version 3.3.3 (R Development Core Team, 2017), and heatmaps were generated using the pheatmap package in R[95].

Supplementary Material

Refer to Web version on PubMed Central for supplementary material.

Acknowledgements

We would like to thank Patricia D'Arcy, Geneviève Perreault, and the animal facility staff at McGill for their excellent care of our animal colony, Katrin Mayer-Barber (NIH, USA) for technical advice on myeloid cell stimulations, Nicolas van Panhuys (Sidra Medical and Research Center, Qatar) for helpful discussions, and Jamie Lee (Mayo Clinic, USA) for the Eo-cre mice and Janis Burkhardt (U Penn, USA) for the LifeAct-GFP mice. Influenza A virus was kindly provided by The Centre for Phenogenomics McGill facility. We would like to thank Helen Matthews and Pam Angelus for clinical support at NIH. Ronald Germain (NIH), Susan Schwab (NYU), Martin Richer (McGill), Heather Melichar (University of Montreal), Samantha Gruenheid (McGill) and the Mandl lab provided critical feedback and advice on various manuscript drafts. We would also like to thank the McGill University Cell Vision Core Facility for flow cytometry and single cell analysis, the Life Sciences Complex Advanced BioImaging Facility (ABIF), and the Goodman Cancer Research Centre Histology Core Facility. C.Sc. was funded by the Max E. Binz Fellowship, McGill University Faculty of Medicine., C.Sh. and P.A. was funded by a Fonds de recherche Santé Quebec fellowship., and D.R. was funded by a Tomlinson Doctoral Fellowship. J.N.M. is a Canada Research Chair for immune cell dynamics. This research was supported by a CIHR project grant (201603PJT-364017) and McGill start up funds to J.N.M., an NSERC Discovery Grant to P.W.W. (2017-05005), and by the Intramural Research Programme of NIAID, NIH (D.L.B. and H.C.S.).

Data Availability Statement

The datasets generated during and/or analysed during the current study are available from the corresponding author on reasonable request.

Code Availability Statement

The code generated during the current study is available from the corresponding author on reasonable request.

References

1. Lenardo MJ, Holland SM. Introduction: Continuing insights into the healthy and diseased immune system through human genetic investigation. Immunol Rev 2019, 287(1): 5–8. [PubMed: 30565248]

2. Hanna S, Etzioni A. Leukocyte adhesion deficiencies. Ann N Y Acad Sci 2012, 1250: 50–55. [PubMed: 22276660]

3. Shiow LR, Roadcap DW, Paris K, Watson SR, Grigorova IL, Lebet T, et al. The actin regulator coronin 1A is mutant in a thymic egress-deficient mouse strain and in a patient with severe combined immunodeficiency. Nat Immunol 2008, 9(11): 1307–1315. [PubMed: 18836449]

4. Crequer A, Picard C, Patin E, D'Amico A, Abhyankar A, Munzer M, et al. Inherited MST1 deficiency underlies susceptibility to EV-HPV infections. PLoS One 2012, 7(8): e44010. [PubMed: 22952854]

5. Thrasher AJ, Burns SO. WASP: a key immunological multitasker. Nat Rev Immunol 2010, 10(3): 182–192. [PubMed: 20182458]

6. Kawai T, Malech HL. WHIM syndrome: congenital immune deficiency disease. Curr Opin Hematol 2009, 16(1): 20–26. [PubMed: 19057201]

7. Aydin SE, Kilic SS, Aytekin C, Kumar A, Porras O, Kainulainen L, et al. DOCK8 deficiency: clinical and immunological phenotype and treatment options - a review of 136 patients. J Clin Immunol 2015, 35(2): 189–198. [PubMed: 25627830]

8. Su HC, Jing H, Angelus P, Freeman AF. Insights into immunity from clinical and basic science studies of DOCK8 immunodeficiency syndrome. Immunol Rev 2019, 287(1): 9–19. [PubMed: 30565250]

9. Ruusala A, Aspenstrom P. Isolation and characterisation of DOCK8, a member of the DOCK180-related regulators of cell morphology. FEBS Lett 2004, 572(1-3): 159–166. [PubMed: 15304341]

10. Cote JF. Identification of an evolutionarily conserved superfamily of DOCK180-related proteins with guanine nucleotide exchange activity. J Cell Science 2002, 115(24): 4901–4913. [PubMed: 12432077]

11. Harada Y, Tanaka Y, Terasawa M, Pieczyk M, Habiro K, Katakai T, et al. DOCK8 is a Cdc42 activator critical for interstitial dendritic cell migration during immune responses. Blood 2012, 119(19): 4451–4461. [PubMed: 22461490]

12. Zhang Q, Dove CG, Hor JL, Murdock HM, Strauss-Albee DM, Garcia JA, et al. DOCK8 regulates lymphocyte shape integrity for skin antiviral immunity. J Exp Med 2014, 211(13): 2549–2566. [PubMed: 25422492]

13. Tangye SG, Pillay B, Randall KL, Avery DT, Phan TG, Gray P, et al. Dedicator of cytokinesis 8-deficient CD4(+) T cells are biased to a TH2 effector fate at the expense of TH1 and TH17 cells. J Allergy Clin Immunol 2017, 139(3): 933–949. [PubMed: 27554822]

14. Randall KL, Lambe T, Johnson AL, Treanor B, Kucharska E, Domaschenz H, et al. Dock8 mutations cripple B cell immunological synapses, germinal centers and long-lived antibody production. Nat Immunol 2009, 10(12): 1283–1291. [PubMed: 19898472]

15. Randall KL, Chan SS, Ma CS, Fung I, Mei Y, Yabas M, et al. DOCK8 deficiency impairs CD8 T cell survival and function in humans and mice. J Exp Med 2011, 208(11): 2305–2320. [PubMed: 22006977]

16. Singh AK, Eken A, Fry M, Bettelli E, Oukka M. DOCK8 regulates protective immunity by controlling the function and survival of RORgammat+ ILCs. Nat Commun 2014, 5: 4603. [PubMed: 25091235]

17. Janssen E, Kumari S, Tohme M, Ullas S, Barrera V, Tas JM, et al. DOCK8 enforces immunological tolerance by promoting IL-2 signaling and immune synapse formation in Tregs. JCI Insight 2017, 2(19).

18. Mizesko MC, Banerjee PP, Monaco-Shawver L, Mace EM, Bernal WE, Sawalle-Belohradsky J, et al. Defective actin accumulation impairs human natural killer cell function in patients with dedicator of cytokinesis 8 deficiency. J Allergy Clin Immunol 2013, 131(3): 840–848. [PubMed: 23380217]

19. Shiraishi A, Uruno T, Sanematsu F, Ushijima M, Sakata D, Hara T, et al. DOCK8 Protein Regulates Macrophage Migration through Cdc42 Protein Activation and LRAP35a Protein Interaction. J Biol Chem 2017, 292(6): 2191–2202. [PubMed: 28028174]

20. Jabara HH, McDonald DR, Janssen E, Massaad MJ, Ramesh N, Borzutzky A, et al. DOCK8 functions as an adaptor that links TLR-MyD88 signaling to B cell activation. Nat Immunol 2012, 13(6): 612–620. [PubMed: 22581261]

21. Janssen E, Tohme M, Hedayat M, Leick M, Kumari S, Ramesh N, et al. A DOCK8-WIP-WASp complex links T cell receptors to the actin cytoskeleton. J Clin Invest 2016, 126(10): 3837–3851. [PubMed: 27599296]
22. Krishnaswamy JK, Gowthaman U, Zhang B, Mattsson J, Szeponik L, Liu D, Wu R, White T, Calabro S, Xu L, Collet MA, Yurieva M, Alsén S, Fogelstrang P, Walter A, Heath WR, Mueller SN, Yrlid U, Williams A, Eisenbarth SC Migratory CD11b+ conventional dendritic cells induce T follicular helper cell-dependent antibody responses. Science Immunol 2017, 2: 1–13.
23. Gowthaman U, Chen JS, Zhang B, Flynn WF, Lu Y, Song W, et al. Identification of a T follicular helper cell subset that drives anaphylactic IgE. Science 2019.
24. Iwasaki A, Foxman EF, Molony RD. Early local immune defences in the respiratory tract. Nat Rev Immunol 2017, 17(1): 7–20. [PubMed: 27890913]
25. Pulendran B, Artis D. New paradigms in type 2 immunity. Science 2012, 337(6093): 431–435. [PubMed: 22837519]
26. Walker JA, McKenzie ANJ. TH2 cell development and function. Nat Rev Immunol 2018, 18(2): 121–133. [PubMed: 29082915]
27. Allen JE, Sutherland TE. Host protective roles of type 2 immunity: parasite killing and tissue repair, flip sides of the same coin. Semin Immunol 2014, 26(4): 329–340. [PubMed: 25028340]
28. Van Dyken SJ, Locksley RM. Interleukin-4- and interleukin-13-mediated alternatively activated macrophages: roles in homeostasis and disease. Annu Rev Immunol 2013, 31: 317–343. [PubMed: 23298208]
29. Palm NW, Rosenstein RK, Medzhitov R. Allergic host defences. Nature 2012, 484(7395): 465–472. [PubMed: 22538607]
30. Paul WE, Zhu J. How are T(H)2-type immune responses initiated and amplified? Nat Rev Immunol 2010, 10(4): 225–235. [PubMed: 20336151]
31. van Panhuys N TCR Signal Strength Alters T-DC Activation and Interaction Times and Directs the Outcome of Differentiation. Front Immunol 2016, 7: 6. [PubMed: 26834747]
32. Halim TY, Steer CA, Matha L, Gold MJ, Martinez-Gonzalez I, McNagny KM, et al. Group 2 innate lymphoid cells are critical for the initiation of adaptive T helper 2 cell-mediated allergic lung inflammation. Immunity 2014, 40(3): 425–435. [PubMed: 24613091]
33. Van Dyken SJ, Nussbaum JC, Lee J, Molofsky AB, Liang HE, Pollack JL, et al. A tissue checkpoint regulates type 2 immunity. Nat Immunol 2016, 17(12): 1381–1387. [PubMed: 27749840]
34. Rohatgi S, Pirofski LA. Host immunity to Cryptococcus neoformans. Future Microbiol 2015, 10(4): 565–581. [PubMed: 25865194]
35. Mody CH, Lipscomb MF, Street NE, Toews GB Depletion of $CD4^+$ (L3T4+) lymphocytes in vivo impairs murine host defense to Cryptococcus neoformans. J Immunol 1990, 144(4): 1472–1477. [PubMed: 1968080]
36. Kawakami K, Qureshi MH, Zhang T, Koguchi Y, Xie Q, Kurimoto M, Saito A Interleukin-4 weakens host resistance to pulmonary and disseminated cryptococcal infection caused by combined treatment with interferon-gamma-inducing cytokines. Cellular Immunology 1999, 197: 55–61. [PubMed: 10555996]
37. Müller U, Stenzel W, Köhler G, Werner C, Polte T, Hansen G, et al. IL-13 Induces Disease-Promoting Type 2 Cytokines, Alternatively Activated Macrophages and Allergic Inflammation during Pulmonary Infection of Mice with Cryptococcus neoformans. J Immunol 2007, 179(8): 5367–5377. [PubMed: 17911623]
38. Sionov E, Mayer-Barber KD, Chang YC, Kauffman KD, Eckhaus MA, Salazar AM, et al. Type I IFN Induction via Poly-ICLC Protects Mice against Cryptococcosis. PLoS Pathog 2015, 11(8): e1005040. [PubMed: 26252005]
39. Xu X, Han L, Zhao G, Xue S, Gao Y, Xiao J, et al. LRCH1 interferes with DOCK8-Cdc42-induced T cell migration and ameliorates experimental autoimmune encephalomyelitis. J Exp Med 2017, 214(1): 209–226. [PubMed: 28028151]
40. Anderson KG, Mayer-Barber K, Sung H, Beura L, James BR, Taylor JJ, et al. Intravascular staining for discrimination of vascular and tissue leukocytes. Nat Protoc 2014, 9(1): 209–222. [PubMed: 24385150]

41. Keles S, Charbonnier LM, Kabaleeswaran V, Reisli I, Genel F, Gulez N, et al. Dedicator of cytokinesis 8 regulates signal transducer and activator of transcription 3 activation and promotes TH17 cell differentiation. J Allergy Clin Immunol 2016, 138(5): 1384–1394 e1382. [PubMed: 27350570]
42. Lloyd CM, Snelgrove RJ. Type 2 immunity: Expanding our view. Sci Immunol 2018, 3(25).
43. McCubbrey AL, Allison KC, Lee-Sherick AB, Jakubzick CV, Janssen WJ. Promoter Specificity and Efficacy in Conditional and Inducible Transgenic Targeting of Lung Macrophages. Front Immunol 2017, 8: 1618. [PubMed: 29225599]
44. Rodero MP, Poupel L, Loyher PL, Hamon P, Licata F, Pessel C, et al. Immune surveillance of the lung by migrating tissue monocytes. Elife 2015, 4: e07847. [PubMed: 26167653]
45. Galluzzi L, Vitale I, Aaronson SA, Abrams JM, Adam D, Agostinis P, et al. Molecular mechanisms of cell death: recommendations of the Nomenclature Committee on Cell Death 2018. Cell Death Differ 2018, 25(3): 486–541. [PubMed: 29362479]
46. Man SM, Kanneganti TD. Converging roles of caspases in inflammasome activation, cell death and innate immunity. Nat Rev Immunol 2016, 16(1): 7–21. [PubMed: 26655628]
47. Helft J, Bottcher J, Chakravarty P, Zelenay S, Huotari J, Schraml BU, et al. GM-CSF Mouse Bone Marrow Cultures Comprise a Heterogeneous Population of CD11c(+)MHCII(+) Macrophages and Dendritic Cells. Immunity 2015, 42(6): 1197–1211. [PubMed: 26084029]
48. Caserta TM, Smith AN, Gultice AD, Reedy MA, Brown TL Q-VD-OPh, a broad spectrum caspase inhibitor with potent antiapoptotic properties. Apoptosis 2003, 8: 345–352. [PubMed: 12815277]
49. Savetsky IL, Ghanta S, Gardenier JC, Torrisi JS, Garcia Nores GD, Hespe GE, et al. Th2 cytokines inhibit lymphangiogenesis. PLoS One 2015, 10(6): e0126908. [PubMed: 26039103]
50. Ben-Sasson SZ, Hu-Li J, Quiel J, Cauchetaux S, Ratner M, Sharpira I, Dinarello CA, Paul WE IL-1 acts directly on CD4 T cells to enhance their antigen-driven expansion and differentiation. Proc Natl Acad Sci U S A 2009, 106(17): 7119–7124. [PubMed: 19359475]
51. Willart MA, Deswarte K, Pouliot P, Braun H, Beyaert R, Lambrecht BN, et al. Interleukin-1alpha controls allergic sensitization to inhaled house dust mite via the epithelial release of GM-CSF and IL-33. J Exp Med 2012, 209(8): 1505–1517. [PubMed: 22802353]
52. Mortha A, Chudnovskiy A, Hashimoto D, Bogunovic M, Spencer SP, Belkaid Y, et al. Microbiota-dependent crosstalk between macrophages and ILC3 promotes intestinal homeostasis. Science 2014, 343(6178): 1249288. [PubMed: 24625929]
53. Lukens JR, Barr MJ, Chaplin DD, Chi H, Kanneganti TD. Inflammasome-derived IL-1beta regulates the production of GM-CSF by CD4(+) T cells and gammadelta T cells. J Immunol 2012, 188(7): 3107–3115. [PubMed: 22345669]
54. Rosen LB, Freeman AF, Yang LM, Jutivorakool K, Olivier KN, Angkasekwinai N, et al. Anti-GM-CSF autoantibodies in patients with cryptococcal meningitis. J Immunol 2013, 190(8): 3959–3966. [PubMed: 23509356]
55. Saijo T, Chen J, Chen SCA, Rosen LB, Yi J, Sorrell TC, Bennett JE, Holland SM, Browne SK, Kwon-Chung KJ Anti-granulocyte-macrophage colony-stimulating factor autoantibodies are a risk factor for central nervous system infection by Cryptococcus gattii in otherwise immunocompetent patients. MBio 2014, 5(2): e00912–00914. [PubMed: 24643864]
56. Chen GH, Olszewski MA, McDonald RA, Wells JC, Paine R 3rd, Huffnagle GB, et al. Role of granulocyte macrophage colony-stimulating factor in host defense against pulmonary Cryptococcus neoformans infection during murine allergic bronchopulmonary mycosis. Am J Pathol 2007, 170(3): 1028–1040. [PubMed: 17322386]
57. Deepe GS Jr., Gibbons R, Woodward E. Neutralization of endogenous granulocyte-macrophage colony-stimulating factor subverts the protective immune response to Histoplasma capsulatum. J Immunol 1999, 163(9): 4985–4993. [PubMed: 10528203]
58. Paine R 3rd, Preston AM, Wilcoxen S, Jin H, Siu BB, Morris SB, et al. Granulocyte-macrophage colony-stimulating factor in the innate immune response to Pneumocystis carinii pneumonia in mice. J Immunol 2000, 164(5): 2602–2609. [PubMed: 10679099]
59. El-Behi M, Ciric B, Dai H, Yan Y, Cullimore M, Safavi F, et al. The encephalitogenicity of T(H)17 cells is dependent on IL-1- and IL-23-induced production of the cytokine GM-CSF. Nat Immunol 2011, 12(6): 568–575. [PubMed: 21516111]

60. Khameneh HJ, Isa SA, Min L, Nih FW, Ruedl C. GM-CSF signalling boosts dramatically IL-1 production. PLoS One 2011, 6(7): e23025. [PubMed: 21829580]
61. Renkawitz J, Kopf A, Stopp J, de Vries I, Driscoll MK, Merrin J, et al. Nuclear positioning facilitates amoeboid migration along the path of least resistance. Nature 2019.
62. Weber A, Wasiliew P, Kracht M. Interleukin-1 (IL-1) pathway. Sci Signal 2010, 3(105): cm1. [PubMed: 20086235]
63. Coccia M, Harrison OJ, Schiering C, Asquith MJ, Becher B, Powrie F, et al. IL-1βeta mediates chronic intestinal inflammation by promoting the accumulation of IL-17A secreting innate lymphoid cells and CD4(+) Th17 cells. J Exp Med 2012, 209(9): 1595–1609. [PubMed: 22891275]
64. Sutton C, Brereton C, Keogh B, Mills KH, Lavelle EC. A crucial role for interleukin (IL)-1 in the induction of IL-17-producing T cells that mediate autoimmune encephalomyelitis. J Exp Med 2006, 203(7): 1685–1691. [PubMed: 16818675]
65. Sheng W, Yang F, Zhou Y, Yang H, Low PY, Kemeny DM, et al. STAT5 programs a distinct subset of GM-CSF-producing T helper cells that is essential for autoimmune neuroinflammation. Cell Res 2014, 24(12): 1387–1402. [PubMed: 25412660]
66. Becher B, Tugues S, Greter M. GM-CSF: From Growth Factor to Central Mediator of Tissue Inflammation. Immunity 2016, 45(5): 963–973. [PubMed: 27851925]
67. Spath S, Komuczki J, Hermann M, Pelczar P, Mair F, Schreiner B, et al. Dysregulation of the Cytokine GM-CSF Induces Spontaneous Phagocyte Invasion and Immunopathology in the Central Nervous System. Immunity 2017, 46(2): 245–260. [PubMed: 28228281]
68. Hamilton JA. Colony-stimulating factors in inflammation and autoimmunity. Nat Rev Immunol 2008, 8(7): 533–544. [PubMed: 18551128]
69. Happel CS, Stone KD, Freeman AF, Shah NN, Wang A, Lyons JJ, et al. Food allergies can persist after myeloablative hematopoietic stem cell transplantation in dedicator of cytokinesis 8-deficient patients. J Allergy Clin Immunol 2016, 137(6): 1895–1898 e1895. [PubMed: 26827248]
70. Cates EC, Gajewska BU, Goncharova S, Alvarez D, Fattouh R, Coyle AJ, et al. Effect of GM-CSF on immune, inflammatory, and clinical responses to ragweed in a novel mouse model of mucosal sensitization. J Allergy Clin Immunol 2003, 111(5): 1076–1086. [PubMed: 12743573]
71. Ohta K, Yamashita N, Tajima M, Miyasaka T, Nakano J, Nakajima M, et al. Diesel exhaust particulate induces airway hyperresponsiveness in a murine model: essential role of GM-CSF. J Allergy Clin Immunol 1999, 104(5): 1024–1030. [PubMed: 10550748]
72. Stampfli MR, Wiley RE, Neigh GS, Gajewska BU, Lei XF, Snider DP, et al. GM-CSF transgene expression in the airway allows aerosolized ovalbumin to induce allergic sensitization in mice. J Clin Invest 1998, 102(9): 1704–1714. [PubMed: 9802884]
73. Chaisakul J, Hodgson WC, Kuruppu S, Prasongsook N. Effects of Animal Venoms and Toxins on Hallmarks of Cancer. J Cancer 2016, 7(11): 1571–1578. [PubMed: 27471574]
74. Allen JE, Wynn TA. Evolution of Th2 immunity: a rapid repair response to tissue destructive pathogens. PLoS Pathog 2011, 7(5): e1002003. [PubMed: 21589896]
75. Jyonouchi H. Airway epithelium and apoptosis. Apoptosis 1999, 4(6): 407–417. [PubMed: 14634325]
76. Bosurgi L, Cao YG, Cabeza-Cabrerizo M, Tucci A, Hughes LD, Kong Y, et al. Macrophage function in tissue repair and remodeling requires IL-4 or IL-13 with apoptotic cells. Science 2017, 356(6342): 1072–1076. [PubMed: 28495875]
77. Harrison OJ, Linehan JL, Shih HY, Bouladoux N, Han SJ, Smelkinson M, et al. Commensal-specific T cell plasticity promotes rapid tissue adaptation to injury. Science 2019, 363(6422).
78. Juncadella IJ, Kadl A, Sharma AK, Shim YM, Hochreiter-Hufford A, Borish L, et al. Apoptotic cell clearance by bronchial epithelial cells critically influences airway inflammation. Nature 2013, 493(7433): 547–551. [PubMed: 23235830]
79. Sachet M, Liang YY, Oehler R. The immune response to secondary necrotic cells. Apoptosis 2017, 22(10): 1189–1204. [PubMed: 28861714]
80. Medina CB, Mehrotra P, Arandjelovic S, Perry JSA, Guo Y, Morioka S, et al. Metabolites released from apoptotic cells act as tissue messengers. Nature 2020, 580(7801): 130–135. [PubMed: 32238926]

81. Lambrecht BN, Hammad H. The immunology of the allergy epidemic and the hygiene hypothesis. Nat Immunol 2017, 18(10): 1076–1083. [PubMed: 28926539]
82. Caton ML, Smith-Raska MR, Reizis B. Notch-RBP-J signaling controls the homeostasis of CD8− dendritic cells in the spleen. J Exp Med 2007, 204(7): 1653–1664. [PubMed: 17591855]
83. Hennet T, Hagen FK, Tabak LA, Marth JD T-cell-specific deletion of a polypeptide N-acetylgalactosaminyl-transferase gene by site-directed recombination. Proc Natl Acad Sci U S A 1995, 92: 12070–12074. [PubMed: 8618846]
84. Glaccum MB, Stocking KL, Charrier K, Smith JL, Willis CR, Maliszewski C, Livingston DJ, Peschon JJ, Morrissey PJ Phenotypic and functional characterization of mice that lack the type I receptor for IL-1. J Immunol 1997, 159: 3364–3371. [PubMed: 9317135]
85. Parkhurst CN, Yang G, Ninan I, Savas JN, Yates JR 3rd, Lafaille JJ, et al. Microglia promote learning-dependent synapse formation through brain-derived neurotrophic factor. Cell 2013, 155(7): 1596–1609. [PubMed: 24360280]
86. Mombaerts P, Clark AR, Rudnicki MA, Iacomini J, Itohara S, Lafaille JJ, Wang L, Ichikawa Y, Hooper ML, Tonegawa S Mutations in the T-cell antigen receptor genes a and b block thymocyte development at different stages. Nature 1992, 360: 225–231. [PubMed: 1359428]
87. Clausen BE, Burkhardt C, Reith W, Renkawitz R, Förster I Conditional gene targeting in macrophages and granulocytes using LysMcre mice. Transgenic Research 1999, 8: 265–277. [PubMed: 10621974]
88. Doyle AD, Jacobsen EA, Ochkur SI, Willetts L, Shim K, Neely J, et al. Homologous recombination into the eosinophil peroxidase locus generates a strain of mice expressing Cre recombinase exclusively in eosinophils. J Leukoc Biol 2013, 94(1): 17–24. [PubMed: 23630390]
89. Riedl J, Flynn KC, Raducanu A, Gartner F, Beck G, Bosl M, et al. Lifeact mice for studying F-actin dynamics. Nat Methods 2010, 7(3): 168–169. [PubMed: 20195247]
90. Ruest A, Michaud S, Deslandes S, Frost EH. Comparison of the Directigen flu A+B test, the QuickVue influenza test, and clinical case definition to viral culture and reverse transcription-PCR for rapid diagnosis of influenza virus infection. J Clin Microbiol 2003, 41(8): 3487–3493. [PubMed: 12904343]
91. Mayer-Barber KD, Andrade BB, Barber DL, Hieny S, Feng CG, Caspar P, et al. Innate and adaptive interferons suppress IL-1alpha and IL-1beta production by distinct pulmonary myeloid subsets during Mycobacterium tuberculosis infection. Immunity 2011, 35(6): 1023–1034. [PubMed: 22195750]
92. Bajenoff M, Egen JG, Koo LY, Laugier JP, Brau F, Glaichenhaus N, et al. Stromal cell networks regulate lymphocyte entry, migration, and territoriality in lymph nodes. Immunity 2006, 25(6): 989–1001. [PubMed: 17112751]
93. Krishnaswamy JK, Singh A, Gowthaman U, Wu R, Gorrepati P, Sales Nascimento M, et al. Coincidental loss of DOCK8 function in NLRP10-deficient and C3H/HeJ mice results in defective dendritic cell migration. Proc Natl Acad Sci U S A 2015, 112(10): 3056–3061. [PubMed: 25713392]
94. Sixt M, Lämmermann T. In Vitro Analysis of Chemotactic Leukocyte Migration in 3D Environments. In: Wells CM, Parsons M (eds). Cell Migration: Developmental Methods and Protocols. Springer Science, 2011.
95. Raivo K. pheatmap: Pretty Heatmaps. R package version 1.0.8. https://CRAN.R-project.org/package=pheatmap. 2015.

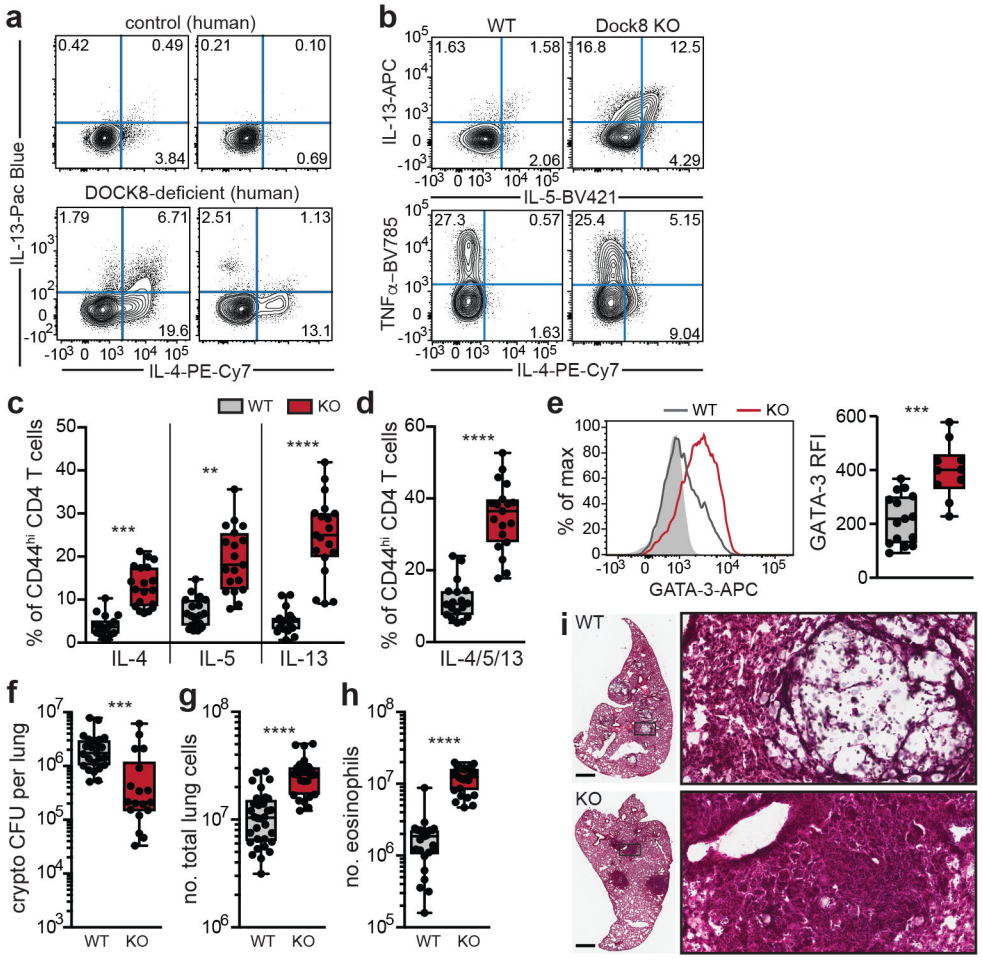

Figure 1. Dock8 deficiency leads to a type-2 immunity bias upon infection.

a, Peripheral blood mononuclear cells from either control or DOCK8-deficient humans restimulated with PMA/ionomycin; data are representative of 4 DOCK8-deficient and 13 healthy humans. **b-d,** Lung cells from wild type (WT) or Dock8 deficient (KO) mice 20 days post *C. neoformans* infection were restimulated *ex vivo* and production of IL-4, IL-5, IL-13, and TNFα assessed by flow cytometry. A representative flow cytometry plot (gated on $CD4^+$ $FoxP3^-$ $CD44^{hi}$ T cells) from a WT and KO mouse where numbers indicate percent cells in each quadrant (**b**). Data are summarized from 4 independent experiments (**c**). Frequency of activated CD4+ T cells making any of the Th2 cytokines IL-4 or IL-5 or IL-13, determined as in (**b,c**) from 4 independent experiments (**d**). **e,** Representative histograms of T helper lineage transcription factor GATA-3 expression measured by flow cytometry in WT naïve ($CD44^{lo}$, shaded) or WT versus KO activated ($CD44^{hi}$) $CD4^+$ T cells in the lung on day 20 post *C. neoformans* infection (left) and summary of relative fluorescent intensity of GATA-3 (RFI) from 3 independent experiments (right). **f-h,** Total *C. neoformans* colony forming units (CFU) in the lung (**f**), and number of total immune cells (**g**) or eosinophils (**h**) in the lung 20 days p.i. with *C. neoformans* compiled from 4-5 independent experiments. **i,** Representative hematoxylin- and eosin-stained lungs of *C. neoformans*-infected lung from WT and KO mice 20 days p.i. Scale bars are 1mm. Insets are magnified 14x. In all graphs error bars represent median ± min/max; each data point is from an individual mouse.

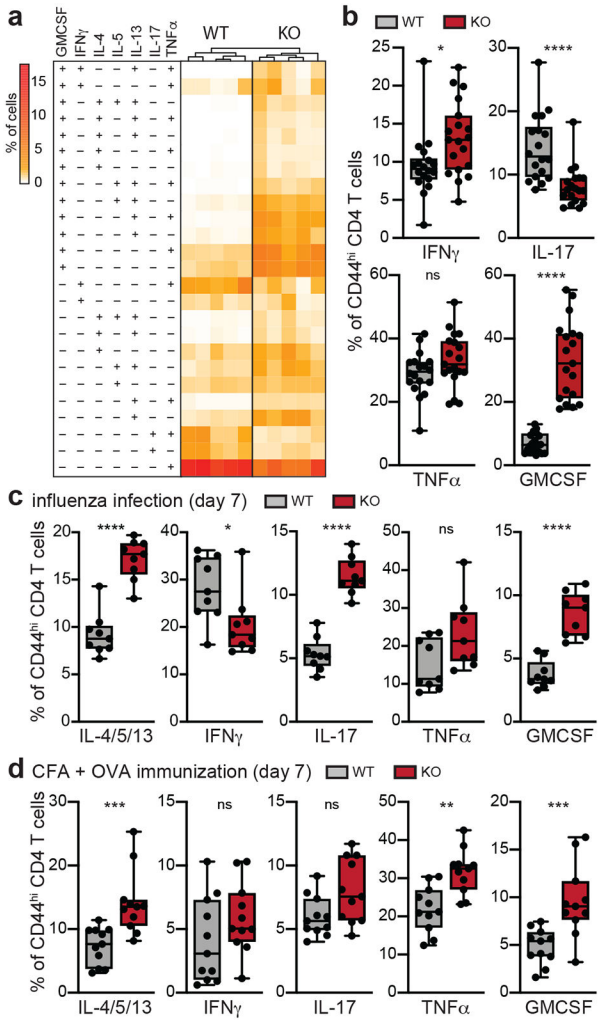

Figure 2. Dock8-deficiency results in a type-2 biased CD4$^+$ T cell response to non-Th2 stimuli and is associated with greater GMCSF production.

a, Heatmap of cytokine combinations (columns) produced by lung CD44^{hi} CD4$_+$ T cells at 20 days p.i. with *C. neoformans* upon *ex vivo* restimulation. Only those combinations differing between WT and KO mice (rows) by more than 0.3 standard deviations of the mean separating WT from KO in an unbiased clustering analysis (dendrogram on right side) are shown. Data are from 5 mice per group. **b,** Frequency of IFNγ, TNFα, IL-17, or GM-CSF producing CD4$^+$ T cells determined as in (**a**) summarized from 4 independent experiments. **c,** Frequency of type-2 cytokine (IL-4, IL-5 or IL-13), IFNγ, IL-17, TNFα, or GM-CSF producing activated CD4$^+$ T cells determined in lungs of mice that were infected intranasally with influenza A virus 7 days prior. **d**, Frequency of type-2 cytokines, IFNγ, IL-17, TNFα, or GM-CSF producing activated CD4$^+$ T cells from mice that were immunized subcutaneously with Complete Freund's adjuvant (CFA) and OVA peptide, measured in the iliac lymph node 7 days later. Data are representative of 4 independent experiments. In all graphs error bars represent median ± min/max; each data point is from an individual mouse.

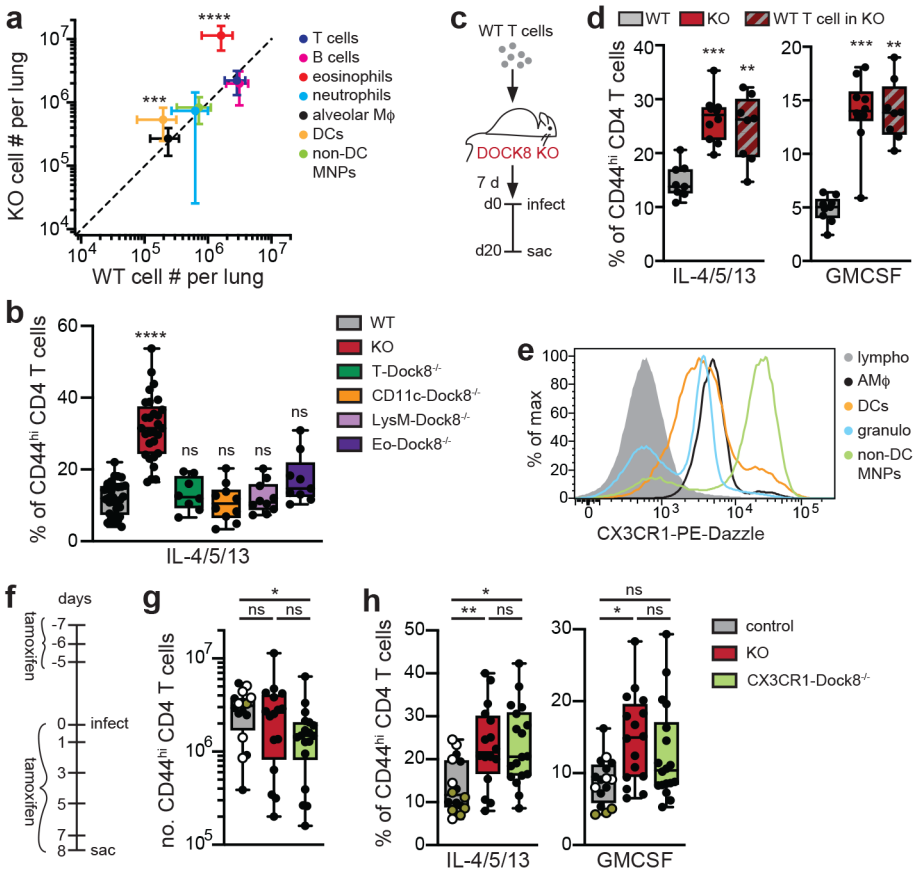

Figure 3. Selective loss of Dock8 in CX3CR1^{+} mononuclear phagocytes recapitulates the type-2 immunity bias.

a, Immune cell population counts found in the lung at day 20 p.i. with *C. neoformans* in WT (x-axis) compared to KO (y-axis) mice, gated as shown in Supplementary Fig. 3b. Dotted line is drawn where WT and KO cell numbers would be equal. Each point represents the mean ± S.D. of 15 (WT) and 17 (KO) mice determined in 3 independent experiments. **b,** Lung cells from WT, KO, or Dock8$^{fl/fl}$ mice crossed to Lck, CD11c, LysM or eosinophil-specific cre lines were harvested 20 days post *C. neoformans* infection, restimulated *ex vivo* and production of IL-4, IL-5, or IL-13 assessed by flow cytometry. **c,d,** Congenically labelled (CD45.1+) T cells from WT mice were transferred into DOCK8 KO (CD45.2+) recipients that were infected with *C. neoformans* 7 days later (**c**) and percent of Th2 cytokine- or GM-CSF- producing CD4^{+} T cells was assessed in 2 independent experiments for WT and KO mice, as well as WT T cells in KO recipients (**d**). **e,** CX3CR1 expression on lung cell populations 20 days post-infection with *C. neoformans* shown as a representative histogram from 3 independent experiments. **f-h,** WT, Dock8 KO, and CX3CR1-Dock8$^{-/-}$ mice were infected with *C. neoformans*, with a tamoxifen treatment schedule as shown (**f**). Number of activated CD4^{+} T cells (**g**) and frequency of type-2 cytokine and GMCSF producing lung CD4^{+} T cells (**h**) measured 8 days post-infection. Control group includes: WT mice (black circles), corn-oil treated Dock8$^{fl/fl}$.CX3CR1-ERcre+ (white circles), and tamoxifen-treated Dock8$^{fl/fl}$.CX3CR1-ERcre− (gold circles). Data are from 3 independent

experiments. In all graphs except (a), error bars represent median ± min/max; each data point is from an individual mouse.

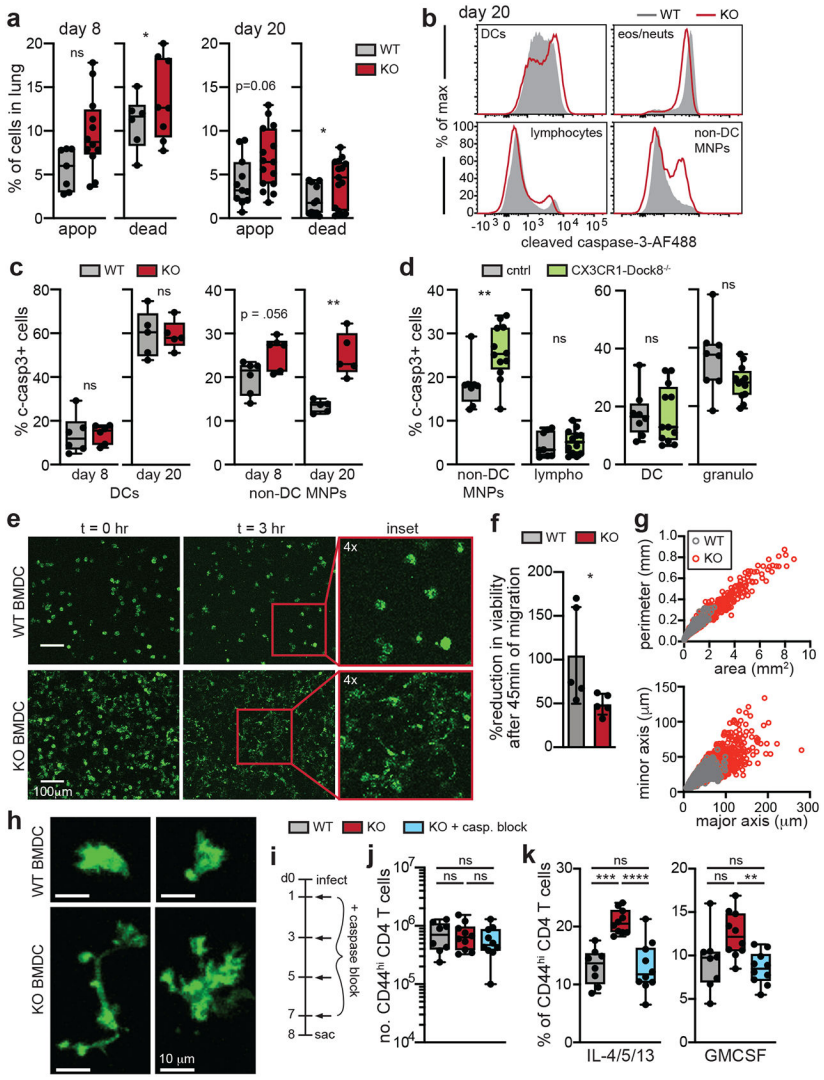

Figure 4. Mononuclear phagocytes lacking Dock8 are highly sensitive to migration-induced shattering, caspase activation and death.

a, Percent of immune cells undergoing apoptosis (apop, AnnexinV+) or are dead (AnnexinV−, viability stain+) in the lung on day 8 or 20 post *C. neoformans* infection. Data from 2-3 independent experiments. **b-d**, Frequency of cleaved caspase-3+ cells analyzed by flow cytometry 8 or 20 days post-infection with *C. neoformans* in DCs, granulocytes, lymphocytes and non-DC MNPs (gated as in Supplementary Fig. 3b). Representative histograms from day 20 (**b**) and data summarized from 2 independent experiments for DCs and non-DC MNPs in WT and KO mice (**c**), and data from CX3CR1-*Dock8*$^{-/-}$ mice or controls treated as in Fig. 3f (d). **e-h,** WT and KO LifeAct-GFP+ BMDCs migrating in a 1.7mg/ml collagen matrix *ex vivo*. Still images taken at 0 and 3 hours from two representative movies, Supplementary Video 2 **(e**). Relative viability measured 45 min from start of migration assay as compared to cells kept in media for the same duration in 2 independent experiments (**f**). BMDC cell area, perimeter, major and minor axes quantified after 3 hours of migration, summarized from 5 movies and 3 mice per group; n=2106 WT, n=4479 KO cells (**g**). Example confocal images of individual WT and KO BMDCs (**h**). **i-k,**

Dock8$^{-/-}$ mice were treated with a pan-caspase inhibitor (Q-VD-OPh) on day 1, 3, 5, and 7 post *C. neoformans* infection (**i**), and on day 8 post infection number of activated (CD44^{hi}) CD4^{+} T cells (**j**) and frequency of activated CD4^{+} T cells making Th2 cytokines (IL-4, IL-5 or IL-13) or GM-CSF following *ex vivo* restimulation (**k**) was assessed in the lung. Data from 2 independent experiments. In all graphs error bars represent median ± min/max except in (**f**) where mean ± SD is shown; each data point is from an individual mouse except in (**g**) where each data point is from an individual cell.

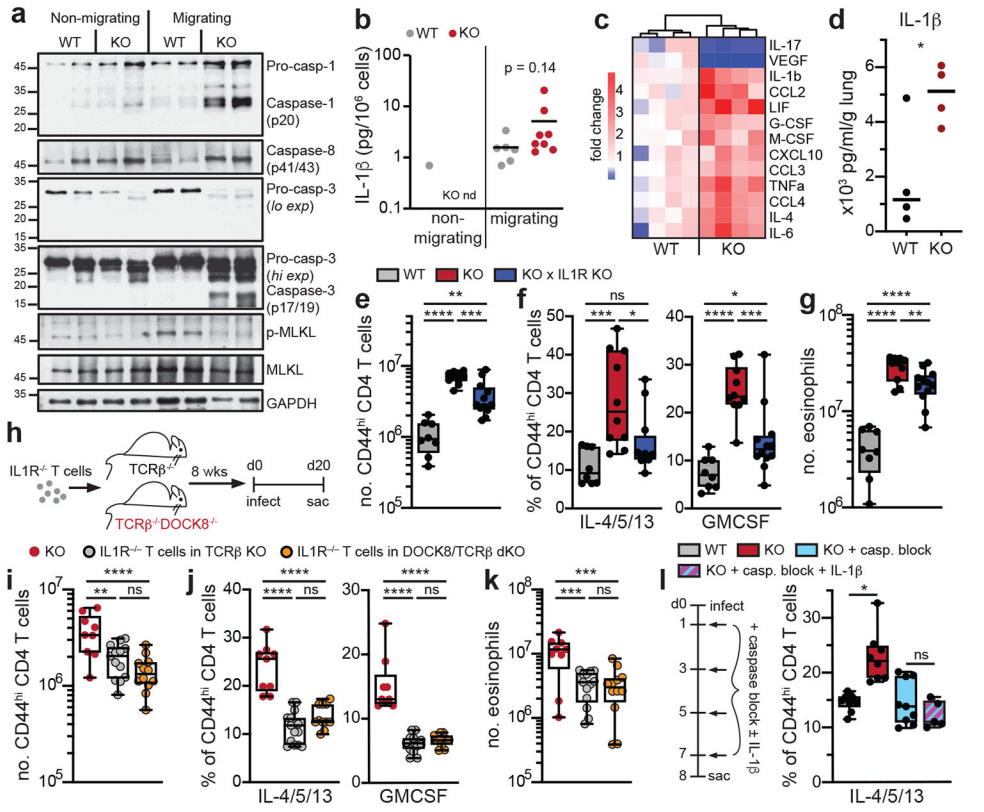

Figure 5. Increased IL-1β is a necessary but not sufficient signal in the greater GM-CSF and type-2 cytokine production by CD4$^+$ T cells in Dock8-deficiency.

a,b, BMDC were kept in dissociated culture (non-migrating) or added to 1.7mg/ml collagen matrices. Caspase and MLKL activation was examined after 40 min by western blot. Pro-caspase 3 gel is shown at high and low exposure (*hi exp, lo exp*). Two independent replicates are shown per group (**a**). IL-1β released was quantified after 3 hours by ELISA in 2 independent experiments. Each data point represents a BMDC batch generated from an individual mouse (**b**). **c-d,** Cytokine production was measured in mice infected with *C. neoformans* (day 20) either in BAL fluid by cytokine array (**c**) or in whole lung by ELISA (**d**). Data in (**c**) is from 4 mice per group and shown as fold change relative to WT group mean. Data in (**d**) is from 2 independent experiments. **e-g,** WT, KO and Dock8/IL-1R double KO mice (KO x IL1R KO) were infected with *C. neoformans* and on day 20 post infection number of activated (CD44^{hi}) CD4$^+$ T cells (**e**), frequency of activated CD4$^+$ T cells making Th2 cytokines (IL-4, IL-5 or IL-13) or GM-CSF following *ex vivo* restimulation (**f**), and eosinophil numbers (**g**) were evaluated in the lung. Data are from 2 independent experiments. **h-k,** Congenically labelled (CD45.2+) T cells from IL1R KO mice were transferred into CD45.1+ TCRβ KO or Dock8/TCRβ double KO recipients that were infected with *C. neoformans* (**h**) and on day 20 p.i. number of activated (CD44^{hi}) CD4$^+$ T cells (**i**), frequency of activated CD4$^+$ T cells making Th2 cytokines (IL-4, IL-5 or IL-13) or GM-w *ex vivo* restimulation (**j**), and eosinophil numbers in the lung was assessed in both recipient groups compared to *Dock8*$^{-/-}$ mice (**k**). Data are from 3 independent experiments. **l,** *Dock8*$^{-/-}$ mice were treated with a pan-caspase inhibitor (Q-VD-OPh) with or without IL-1β on day 1, 3, 5, and 7 post *C. neoformans* infection, and on day 8 post infection the

frequency of activated $CD4^+$ T cells making Th2 cytokines (IL-4, IL-5 or IL-13) following *ex vivo* restimulation was assessed in the lung. Data from 2 independent experiments. For all graphs each data point is from an individual mouse. In (**b,d**) lines represent means; in all other graphs error bars represent median ± min/max.

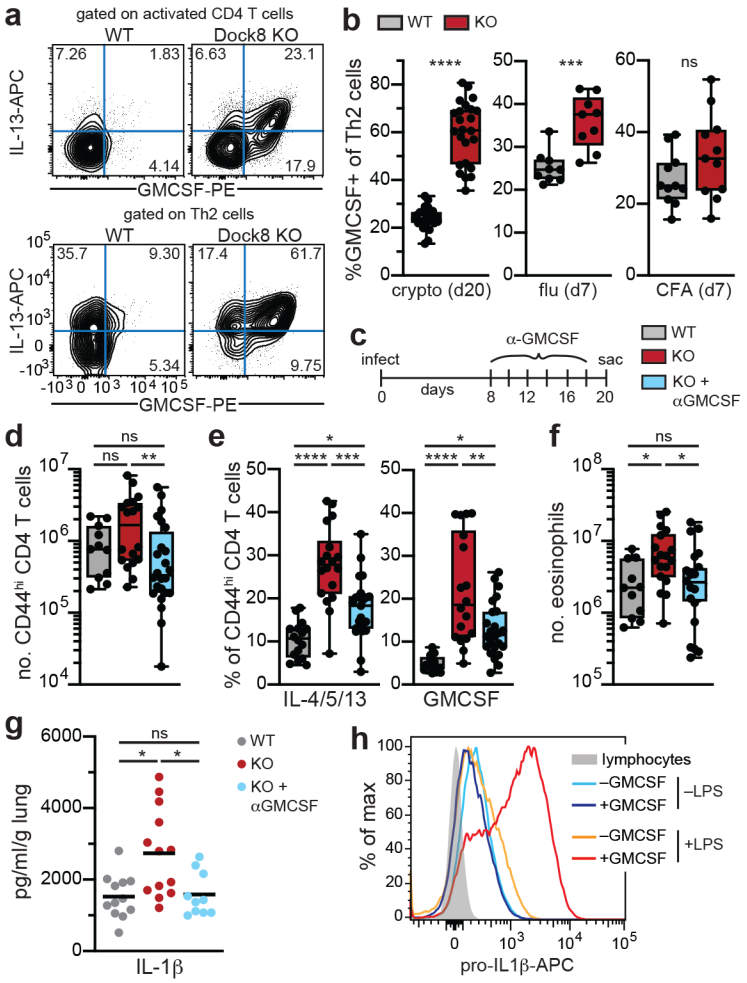

Figure 6. GM-CSF production by CD4$^+$ T cells plays a role in the type-2 bias, amplifying IL-1β production.

a, Lung cells from WT and KO mice 20 days post *C. neoformans* infection were restimulated *ex vivo*, and production of GM-CSF by CD4$^+$ T cells assessed by flow cytometry. Representative flow cytometry plots (gated on CD4$^+$FoxP3$^-$ CD44^{hi} T cells, top) or gated on any Th2 cytokine-producing CD4$^+$ T cells (bottom), with numbers indicating percent cells in each quadrant, are shown. **b,c,** GMCSF-production by CD4$^+$ T cells was determined as in (a) upon infection with *C. neoformans* (lung, day 20 p.i.), influenza A (lung, day 7 p.i.) or following immunization with CFA + OVA (iliac lymph node, day 7 p.i.). and the frequency of GMCSF-producing Th2 cells is summarized from 2-4 independent experiments. **c-f,** KO mice were treated with αGMCSF every 2 days from day 8 post *C. neoformans* infection and compared to untreated KO and WT mice (**c**). On day 20 post infection number of activated (CD44^{hi}) CD4$^+$ T cells (**d**), frequency of activated CD4$^+$ T cells making Th2 cytokines (IL-4, IL-5 or IL-13) or GM-CSF following *ex vivo* restimulation (**e**), eosinophil numbers (**f**) were evaluated in the lung. Data are from 3 independent experiments. **g**, IL-1β production was measured in WT, KO, or KO treated with αGMCSF infected with *C. neoformans* (day 20) either in whole lung by ELISA. **h,** Monocytes were cultured in media with or without GM-CSF in presence or absence of LPS

and protein expression of pro-IL1β measured by flow cytometry. A representative histogram is shown. For all graphs error bars represent median ± min/max, except in (**g**) where group means are shown; each data point is from an individual mouse.

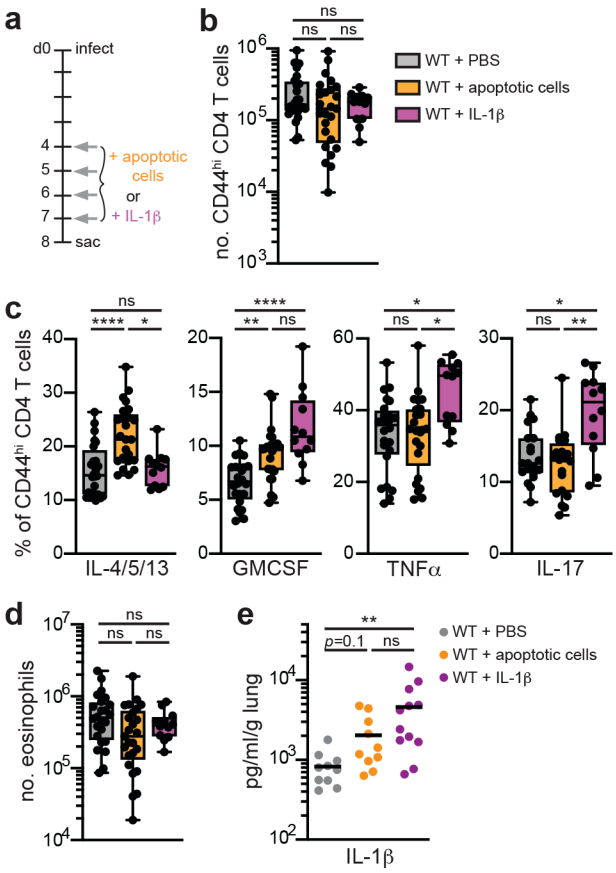

Figure 7. Cell death provides a necessary and sufficient type-2-inducing signal.

a-e, WT mice were infected with *C. neoformans* and given intrapharyngeal IL-1β, 1x10^7 irradiated thymocytes i.v. on days 4, 5, 6, and 7 p.i., or injected with PBS alone, as shown (**a**). The number of activated (CD44^{hi}) CD4$^+$ T cells (**b**), frequency of activated CD4$^+$ T cells making Th2 cytokines (IL-4, IL-5 or IL-13), GM-CSF, TNFα or IL-17 following *ex vivo* restimulation (**c**), and eosinophil numbers (**d**) were evaluated in the lung. Levels of IL-1β were measured in total lung homogenate. Data are from 2-5 independent experiments. For all graphs error bars represent median ± min/max, except in (**e**) group means are shown; each data point is from an individual mouse.